

Calculations for MPGDs

Algorithms to calculate ionisation patterns,
electron and ion transport,
charge deposition

Zaragoza, MPGD 2013

[Four Curies: Pierre, Marie, Irène and
Pierre's father, around 1904 at the BIPM]



1896: Ionisation by radiation

- ▶ Early in the study of radioactivity, ionisation by radiation was recognised:

” Becquerel discovered in 1896 the special radiating properties of uranium and its compounds. Uranium emits very weak rays which leave an impression on photographic plates. These rays pass through black paper and metals; **they make air electrically conductive.** “

[Pierre Curie, Nobel Lecture, June 6th 1905]

“A sphere of charged uranium, which discharges spontaneously in the air under the influence of its own radiation, retains its charge in an absolute vacuum. The exchanges of electrical charges that take place between charged bodies under the influence of the new rays, are the **result of a special conductivity imparted to the surrounding gases**, a conductivity that persists for several moments after the radiation has ceased to act.”

[Antoine Henri Becquerel, Nobel Lecture, December 11th 1903]



1930-1933: EM energy loss

- ▶ 1930 - Hans Bethe, non-relativistic quantum calculation:

The loss in kinetic energy per centimeter path is

$$-\frac{dT}{dx} = N E = \frac{4\pi e^4 z^2 N}{m v^2} \ln \frac{(2) m v^2}{c R \hbar} .$$

Z: “hidden in N ”

(2): only for electrons

R: Rydberg constant

- ▶ 1931 - Christian Møller solves relativistic e^- scattering.
- ▶ 1932 - Hans Bethe, relativistic quantum calculation:

Ein Teilchen der Ladung ez möge sich mit der Geschwindigkeit v durch eine Substanz hindurchbewegen, welche in der Volumeneinheit N Atome der Ordnungszahl Z enthält. Dann verliert das Teilchen pro Zentimeter Weg die Energie

$$-\frac{dT}{dx} = \frac{2\pi e^4 N Z z^2}{m v^2} \left(\lg \frac{2 m v^2 W}{\bar{E}^2 \left(1 - \frac{v^2}{c^2}\right)} - \frac{v^2}{c^2} \right),$$

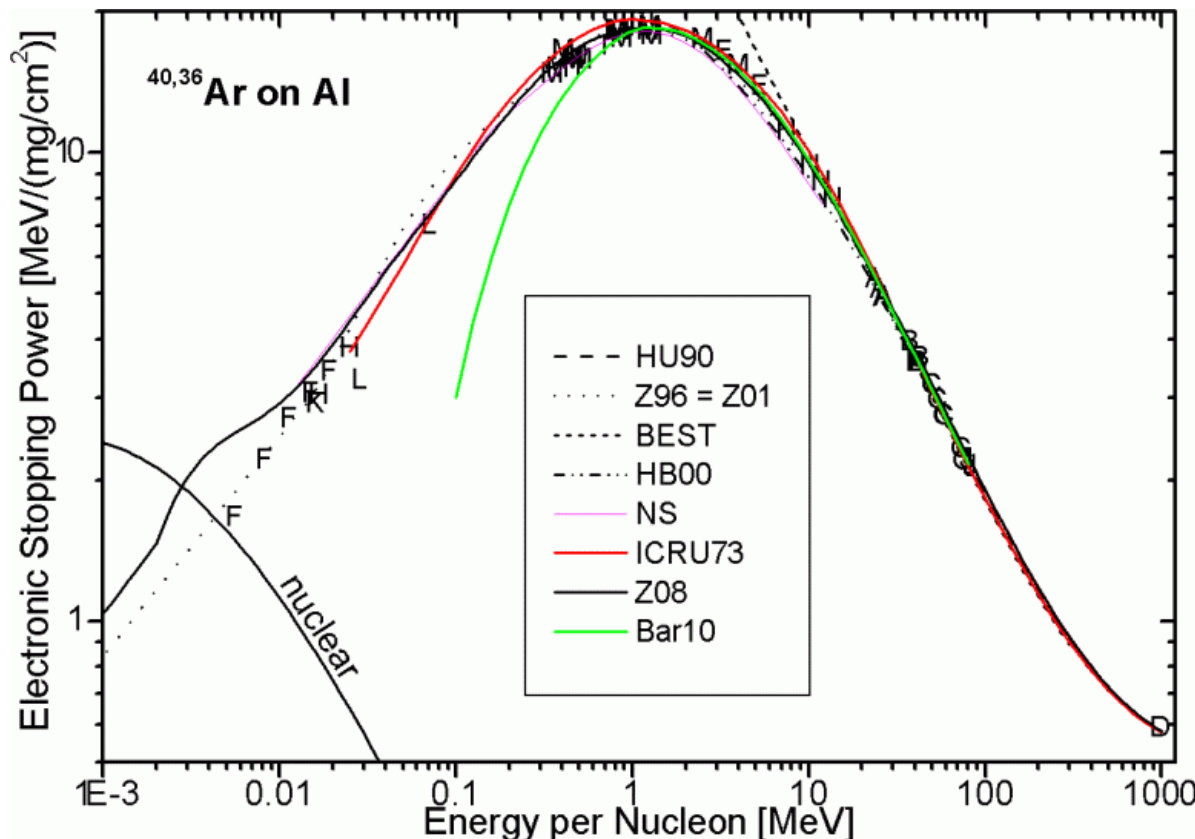
falls wir nur den Energieverlust durch solche Stöße ins Auge fassen, bei denen im einzelnen höchstens die Energie W auf das Atom übertragen wird³⁾.

\bar{E} : average atomic ionisation energy

W : largest energy transfer per collision

Electromagnetic losses at low energy

- ▶ Nuclear effects abound at low energy.
- ▶ Numerous models: SRIM, MSTAR, CasP, PASS ...



- ▶ Ref: Helmut Paul, <http://www.exphys.uni-linz.ac.at/Stopping/>

Лев Давидович Ландау
(1908-1968)



1944: Energy loss fluctuations

- ▶ Given a single-collision energy loss distribution $w(\epsilon)$, the distribution $f(s)$ of the energy loss s after many collisions is *schematically* given by the Laplace transform:

$$L f(x, s) = \bar{f}(x, p) = e^{-x \int_0^\infty (1 - e^{-p\epsilon}) w(\epsilon) d\epsilon}$$

x : direction of travel

$s \leftrightarrow p$: total energy loss

- ▶ Landau showed (1944), assuming in particular:
 - ▶ **thick layers**: numerous small energy losses;
 - ▶ Rutherford-inspired energy loss distribution $w(\epsilon) \sim 1/\epsilon^2$;
 - ▶ neglect of the atomic structure:

$$L f(s) \approx s^s$$

Use with caution !

► 2 GeV protons on an (only !) 5 cm thick Ar gas layer:

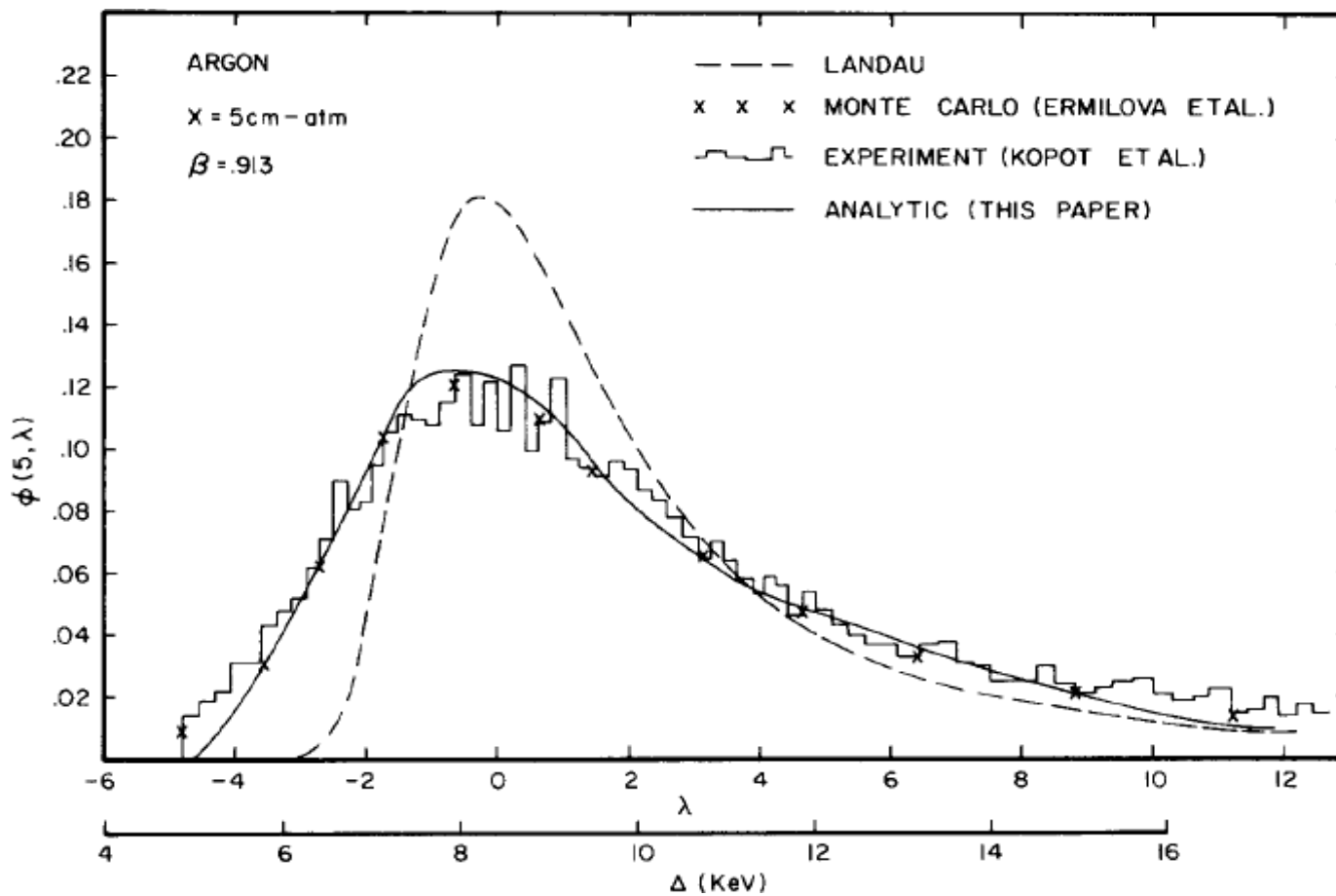


[Diagram: Richard Talman, NIM A 159 (1979) 189-211]

Basics of the PAI model



Wade Allison

John Cobb

► Key ingredient: photo-absorption cross section $\sigma_\gamma(E)$

$$\frac{\beta^2 \pi}{\alpha} \frac{d\sigma}{dE} = \frac{\sigma_\gamma(E)}{E} \log \left(\frac{1}{\sqrt{(1-\beta^2 \epsilon_1)^2 + \beta^4 \epsilon_2^2}} \right) +$$

Cross section to
transfer energy E

$$\frac{1}{N \bar{h} c} \left(\beta^2 - \frac{\epsilon_1}{|\epsilon|^2} \right) \theta +$$

$$\frac{\sigma_\gamma(E)}{E} \log \left(\frac{2 m_e c^2 \beta^2}{E} \right) +$$

$$\frac{1}{E^2} \int_0^E \sigma_\gamma(E_1) dE_1$$

Relativistic rise

Čerenkov radiation

Resonance region

Rutherford scattering

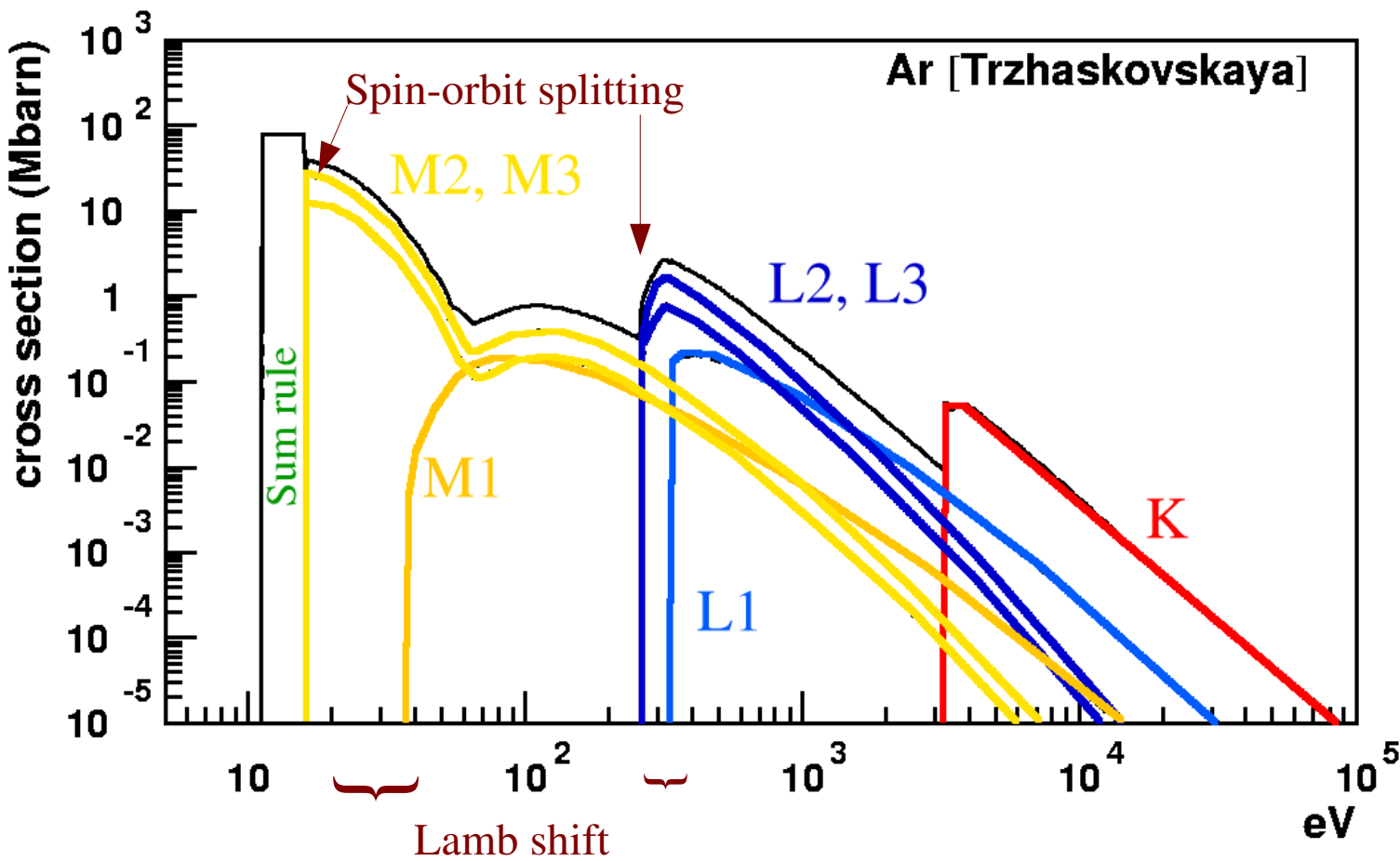
With: $\epsilon_2(E) = \frac{N_e \bar{h} c}{EZ} \sigma_\gamma(E)$

$$\epsilon_1(E) = 1 + \frac{2}{\pi} P \int_0^\infty \frac{x \epsilon_2(x)}{x^2 - E^2} dx$$

$$\theta = \arg(1 - \epsilon_1 \beta^2 + i \epsilon_2 \beta^2) = \frac{\pi}{2} - \arctan \frac{1 - \epsilon_1 \beta^2}{\epsilon_2 \beta^2}$$

Photo-absorption in argon

- Argon has 3 shells, hence 3 groups of lines:



$K = 1s$

$L1 = 2s$

$L2 = 2p\ 1/2$

$L3 = 2p\ 3/2$

$M1 = 3s$

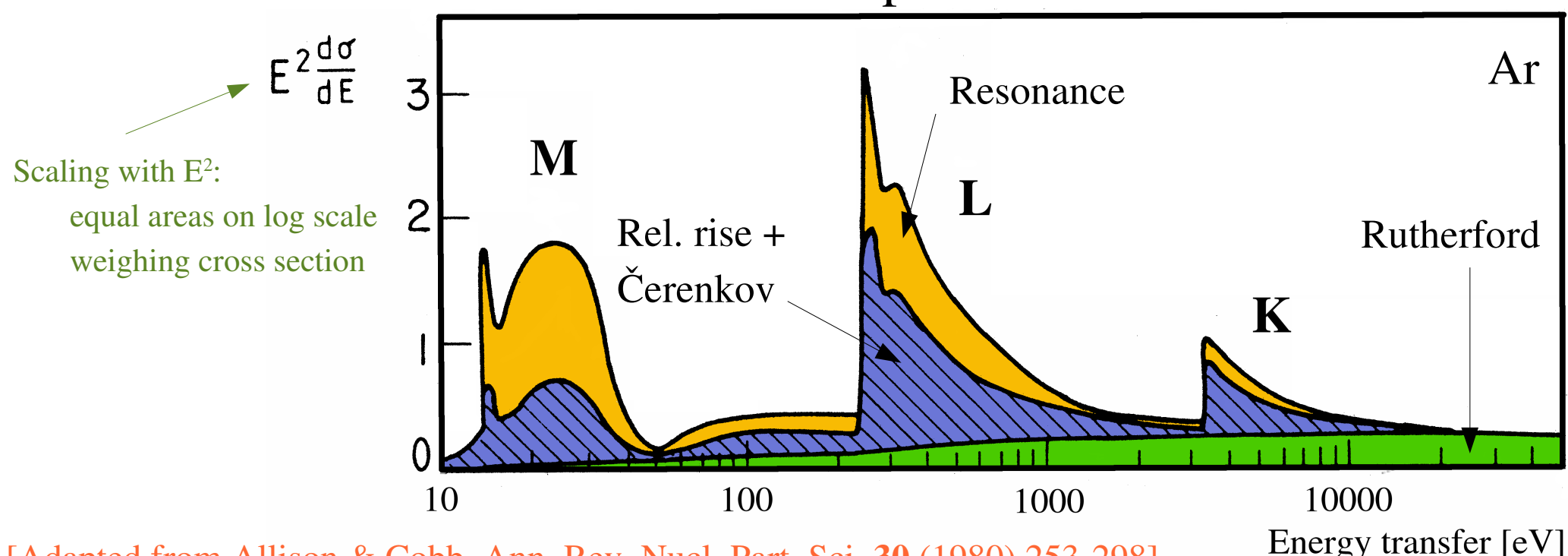
$M2 = 3p\ 1/2$

$M3 = 3p\ 3/2$

[Plot from Igor Smirnov]

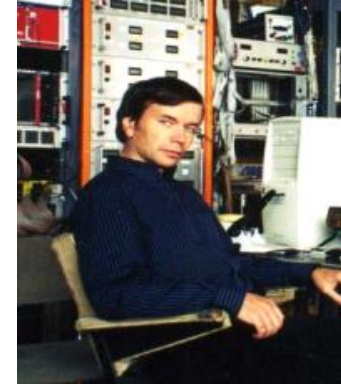
Importance of the PAI model terms

- ▶ All electron orbitals (shells) participate:
 - ▶ outer shells: frequent interactions, few electrons;
 - ▶ inner shells: few interactions, many electrons.
- ▶ All terms in the formula are important.



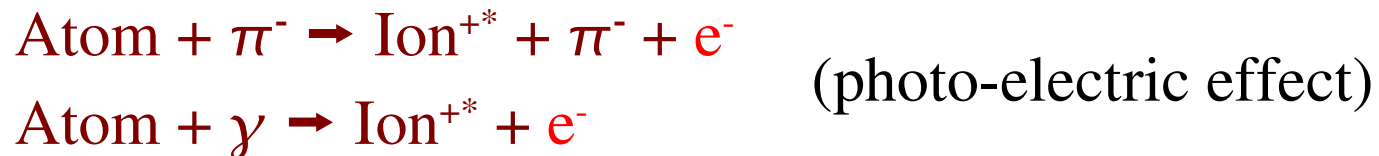
[Adapted from Allison & Cobb, Ann. Rev. Nucl. Part. Sci. 30 (1980) 253-298]

Heed: ionisation Monte Carlo



Igor Smirnov

- ▶ PAI model or absorption of real photons:



- ▶ Decay of excited states:



- ▶ Treatment of:

- ▶ secondary photons, returning to the PAI model,
- ▶ ionising photo-electrons and Auger-electrons,
collectively known as δ -electrons:



De-excitation

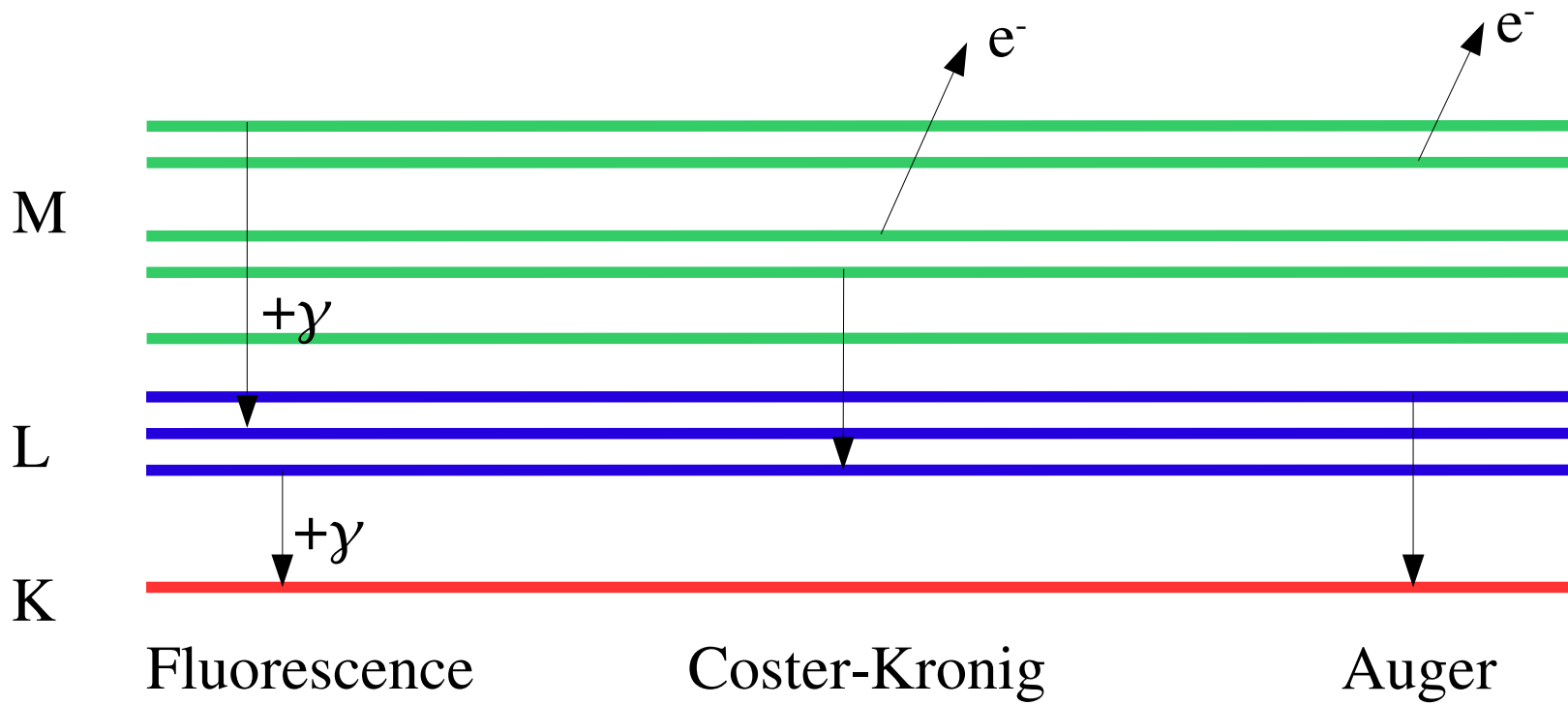


Ralph de Laer Kronig
(1904-1995)

Dirk Coster
(1889-1950)

Lise Meitner
(1878-1968)

Pierre Victor Auger
(1899-1993)



References:

D. Coster and R. de L. Kronig, Physica **2** (1935) 13-24.

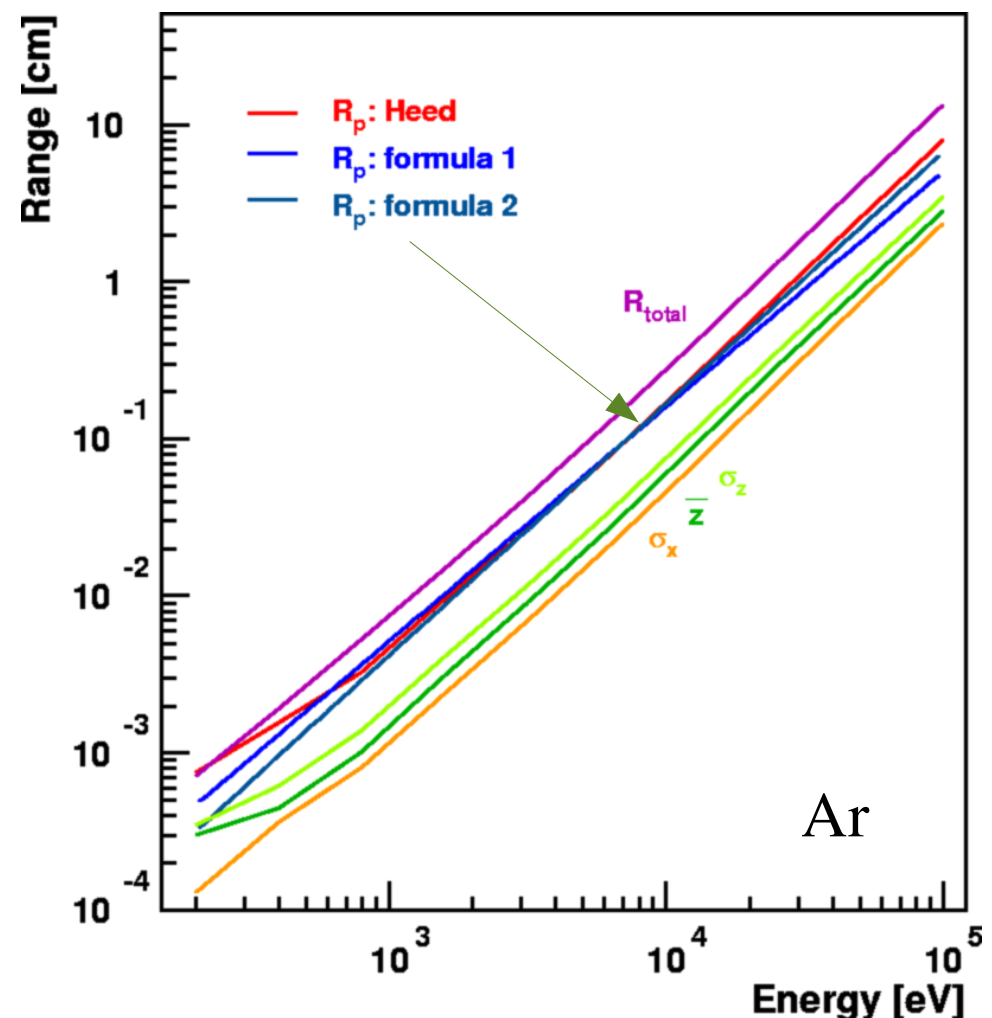
Lise Meitner, *Über die β-Strahl-Spektra und ihren Zusammenhang mit der γ-Strahlung*, Z. Phys. **11** (1922) 35-54.

L. Meitner, *Das β-Strahlenspektrum von UX₁ und seine Deutung*, Z. Phys. **17** (1923) 54-66.

P. Auger, J. Phys. Radium **6** (1925) 205.

Range of photo- and Auger-electrons

- ▶ Electrons scatter in a gas.
- ▶ Measures of the range:
 - ▶ R_{total} total path length
 - ▶ R_p practical range
 - ▶ \bar{z} cog in direction of initial motion
 - ▶ σ_z RMS in direction of initial motion
 - ▶ σ_x RMS transverse to initial motion



Practical range: distance at which the tangent through the inflection point of the descending portion of the depth-absorbed dose curve meets the extrapolation of the Bremsstrahlung background (ICRU report 35, 1984)

Degrad – Steve Biagi

- ▶ Auger cascade model for **electron thermalisation** in gas mixtures produced by photons or particles in electric and magnetic fields.
- ▶ Applications:
 - ▶ **Work function** and **Fano factor** (including shape)
 - ▶ Cloud size after **β -decay**
 - ▶ **Cluster size** & density distribution for charged particle tracks
- ▶ Degrad shares its electron impact cross sections with Magboltz and is a successor to MIP.

The Degrad model

- ▶ Atomic/molecular cascade:
 - ▶ Auger and Coster-Kronig decay; Xe: innermost 17 shells
 - ▶ fluorescence;
 - ▶ outer shell electron shake off.
- ▶ Photon absorption:
 - ▶ photoelectric effect;
 - ▶ Compton scattering.
- ▶ Electron scattering:
 - ▶ rotational, vibrational, excitation and ionisation scattering.
- ▶ Atomic de-excitation:
 - ▶ Penning;
 - ▶ Hornbeck-Molnar.
$$\text{Ar}^* + \text{CO}_2 \rightarrow \text{Ar} + \text{CO}_2^+ + \text{e}^-.$$
$$\text{Ar}^* + \text{Ar} \rightarrow \text{Ar}_2^+ + \text{e}^-.$$
- ▶ Not included:
 - ▶ Bremsstrahlung, pair production.

William Gilbert
(1544-1603)



1600: The force of amber

- ▶ 1544: William Gilbert born in Colchester
- ▶ 1600: *De magnete, magneticisque corporibus,
et de magno magnetе tellure.*
 - ▶ Concluded that the Earth is a magnet;
 - ▶ Credited with the first use of the term “electric force”.

vim illam electricam nobis placet appellare quæ ab humore prouenit

- ▶ 1601: Physician to Elizabeth I and James I.

[Guilielmi Gilberti, *De magnete ...*, excudebat Petrus Short anno MDC, Londini,
courtesy Universidad Complutense de Madrid and Google books]

GREAT has ever been the fame of the loadstone and of amber in the writings of the learned: many philosophers cite the loadstone and also amber whenever, in explaining mysteries, their minds become obfuscated and reason can no farther go.¹

William Gilbert: the *effluvium*

And now, at last, we have to see why corpuscles are drawn toward substances that derive their origin from water,

its force has to be **awakened by friction** till the substance attains a moderate heat, and gives out an **effluvium**, and its surface is made to shine.

All bodies are united and, as it were, cemented together by moisture,
of electrics, being the subtlest matter of solute moisture, attract corpuscles.'

But the peculiar effluvia lay hold of the bodies with which they unite, enfold them, as it were, in their arms, and bring them into union with the electrics; and the bodies are led to the electric source, the effluvia having **greater force the nearer they are to that**.

Effluvium: electric field

Attraction

Relation with distance



1749: 2d flow of liquids

- ▶ Jean le Rond d'Alembert takes part in a hydrodynamics contest in Berlin. Euler gives the price to Jacob Adami.
- ▶ d'Alembert and Euler don't speak for 10 years, but:

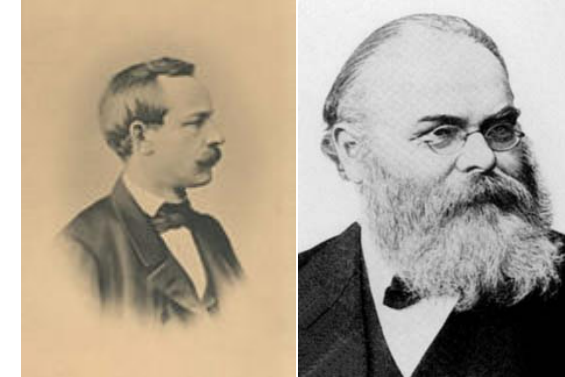
59. On peut encore trouver M & N par la méthode suivante qui est un peu plus simple. Puisque $\frac{dp}{dz} = - \frac{dq}{dx}$ & $\frac{dp}{dx} = \frac{dq}{dz}$, donc $qdz + pdz$ & $pdx - qdx$ seront des différentielles complètes.

J. le Rond d'Alembert, “*Theoria resistentiae quam patitur corpus in fluido motum, ex principiis omnino novis et simplissimus deducta, habita ratione tum velocitatis, figurae, et massae corporis moti, tum densitatis compressionis partium fluidi*” (1749). Manuscript at the Berlin-Brandenburgische Akademie der Wissenschaften as document I-M478.

J. le Rond d'Alembert, “*Essai d'une nouvelle théorie de la résistance des fluides*” (1752) Paris.
Available from Gallica BnF.

Elwin Bruno Christoffel (1829-1900)

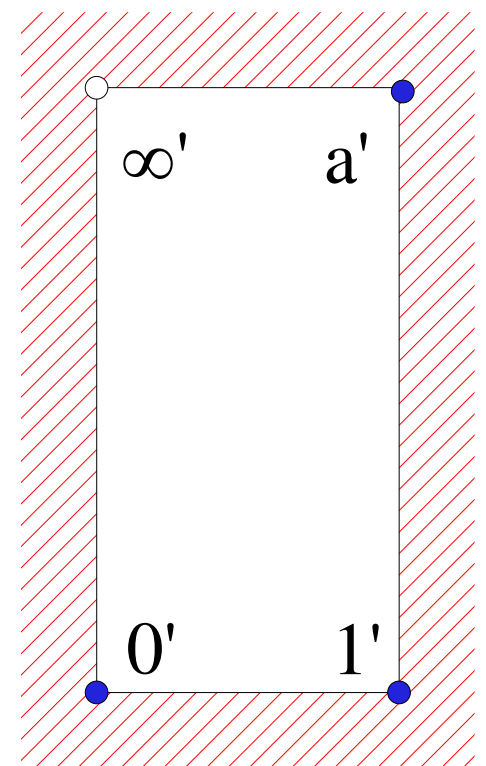
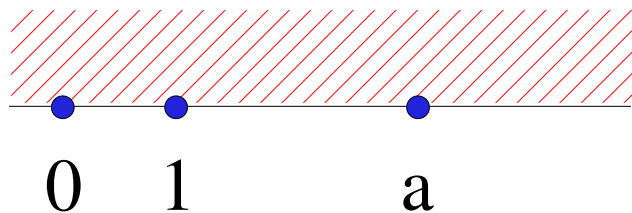
Karl Hermann Amandus Schwarz (1843-1921)



1867: Conformal mappings

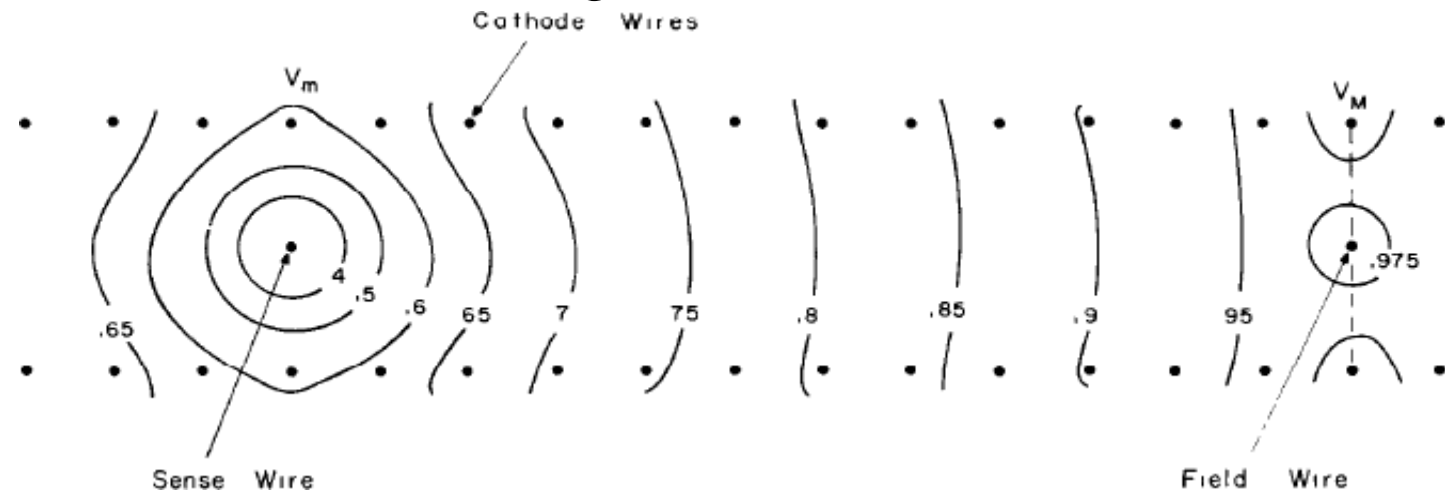
- ▶ Schwartz-Christoffel transformation of a half-plane to the external part of a rectangle:

$$\begin{aligned} z \rightarrow & \int_0^z \frac{d\xi}{\sqrt{\xi(\xi-1)(\xi-a)}} \\ & = \frac{2}{\sqrt{a}} \operatorname{sn}^{-1}\left(\sqrt{z}, \frac{1}{\sqrt{a}}\right) \end{aligned}$$



1970s: Analog method for 2d potentials

- ▶ Equivalent problem approach, still alive in the 1970s:
 - ▶ sheets of carbon paper of ~constant surface resistivity,
 - ▶ electrodes of any shape made with silver paint,
 - ▶ apply suitable boundary potentials,
 - ▶ measure the voltages.



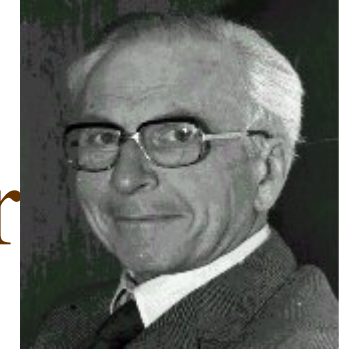
[G. Charpak, F. Sauli and W. Duinker, *High-accuracy drift chambers and their use in strong magnetic fields*, Nuclear Instruments and Methods, **108** (1973) 413-426.]

Why not 3d ?

Caspar Wessel (1745-1818)
Jean-Robert Argand (1768-1822)
Johann Carl Friedrich Gauss (1777-1855)
Sir William Rowan Hamilton (1805-1865)
Charles Sanders Peirce (1839-1914)
Georg Frobenius (1849-1917)

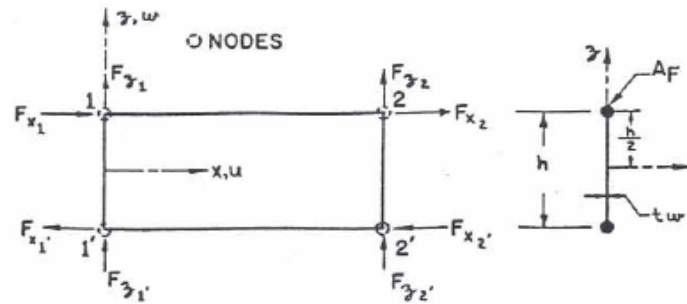


- ▶ The complex numbers $(\mathbb{R}^2, +, \times)$ form a field, like the real numbers $(\mathbb{R}, +, \times)$, but $(\mathbb{R}^3, +, \times)$ does not. As a result, 2d arithmetic can be done with complex numbers, but there is no 3d equivalent for this.
- ▶ It can be proven that only \mathbb{R} and \mathbb{C} can form a commutative division algebra (field).
- ▶ $(\mathbb{R}^4, +, \times)$ can be made into a non-commutative division algebra known as quaternions, but this would not be helpful since $\nabla \cdot E$ links all dimensions.

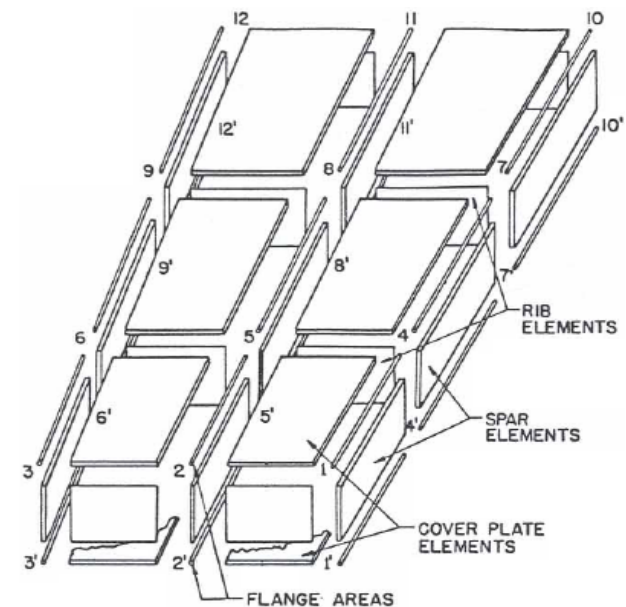


1956: Finite elements by computer

► “*Stiffness and Deflection Analysis of Complex Structures*”, a study in the use of the finite element technique (then called “direct stiffness method”) for aircraft wing design.



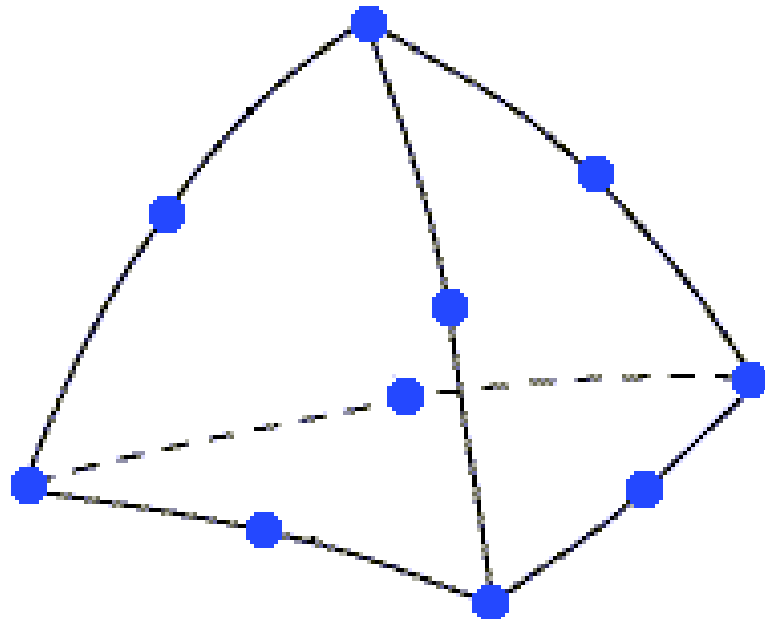
$$[K] = \frac{6EI}{Lh^2(1+4n)} \begin{bmatrix} u_1 & v_1 & w_1 & u_2 & v_2 & w_2 \\ (4/3)(1+n) & 0 & 0 & (4/3)(1+n) & 0 & 0 \\ 0 & -(h/L) & 0 & 0 & 0 & -h^2/L^2 \\ -(h/L) & 0 & h^2/L^2 & 0 & 0 & 0 \\ (2/3)(1-2n) & 0 & 0 & 0 & 0 & 0 \\ h/L & 0 & -h^2/L^2 & h/L & 0 & h^2/L^2 \end{bmatrix}$$



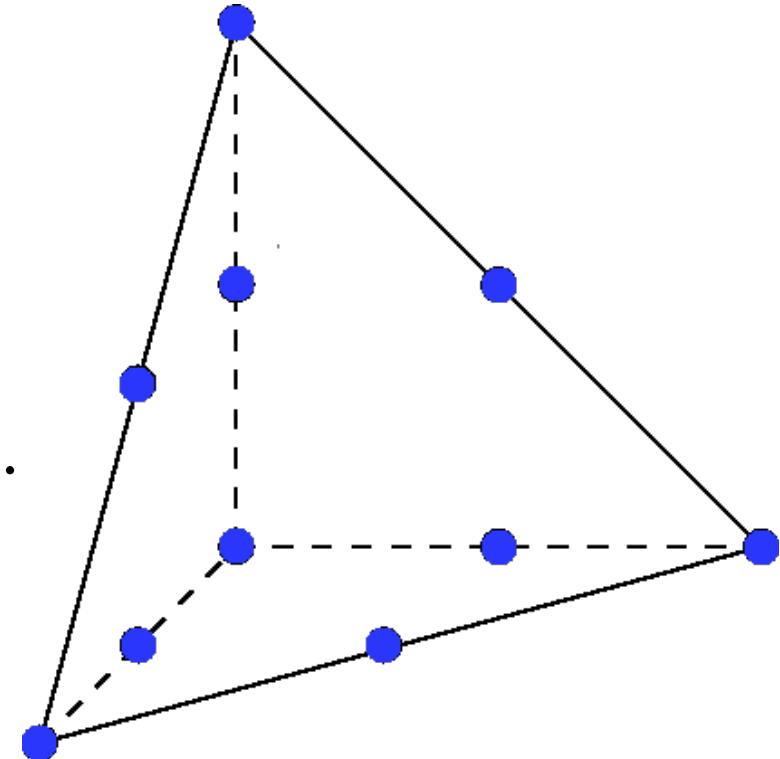
[M.J. Turner, R.W. Clough, H.C. Martin and L.J. Topp, *Stiffness and Deflection Analysis of Complex Structures*, J. Aero. Sc. 23 (1956) 805-824. MJT & LJT and RWC in part were with Boeing. The paper covers work done by 1953.]

Choice of element

- ▶ Many finite element programs offer triangles in 2D and tetrahedra in 3D.

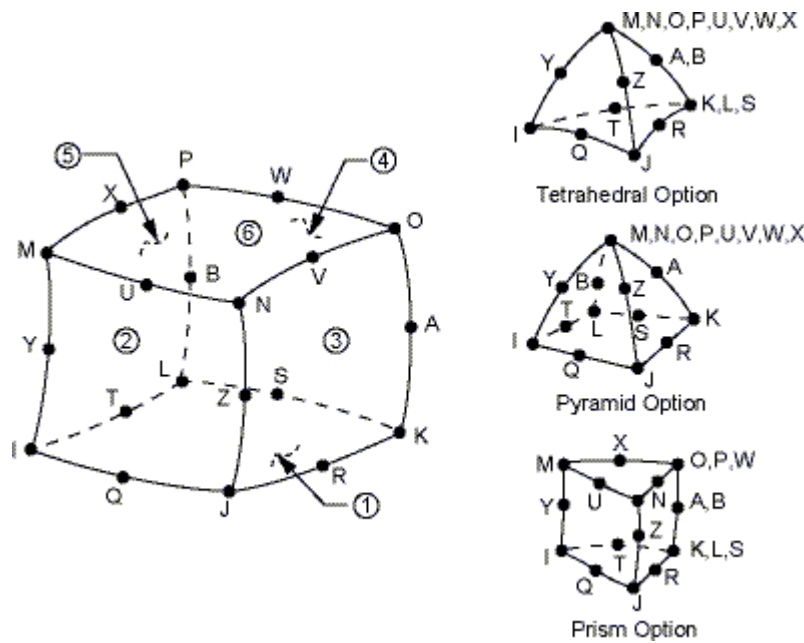
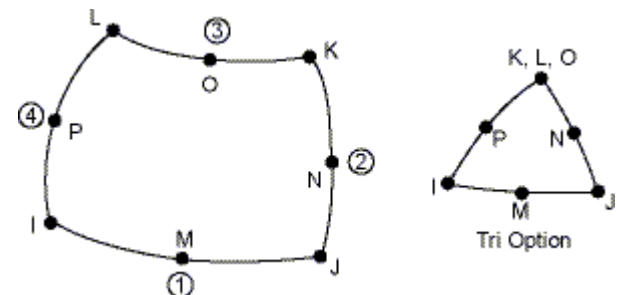


- ▶ **SOLID123** (10 nodes): a feature of ANSYS® is the parabolically curved tetrahedron which adapts well to round surfaces.



Other Ansys elements

- **PLANE121** (8 nodes): the usual Ansys 2D electrostatics element.



- **SOLID122** (20 nodes): an alternative 3D element. No Garfield interface yet.

- Both are from the so-called “serendipity” family.

Open source finite elements

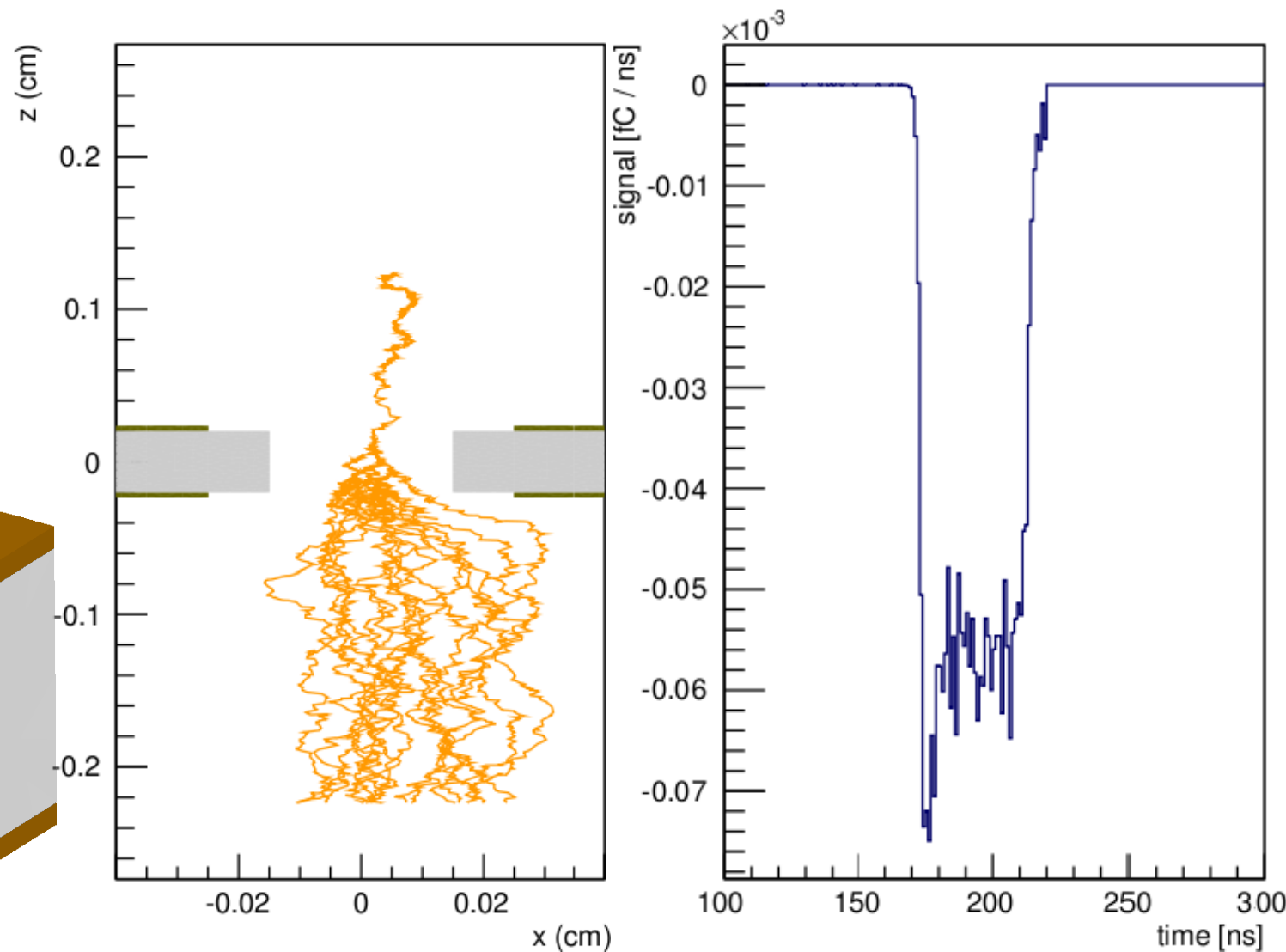
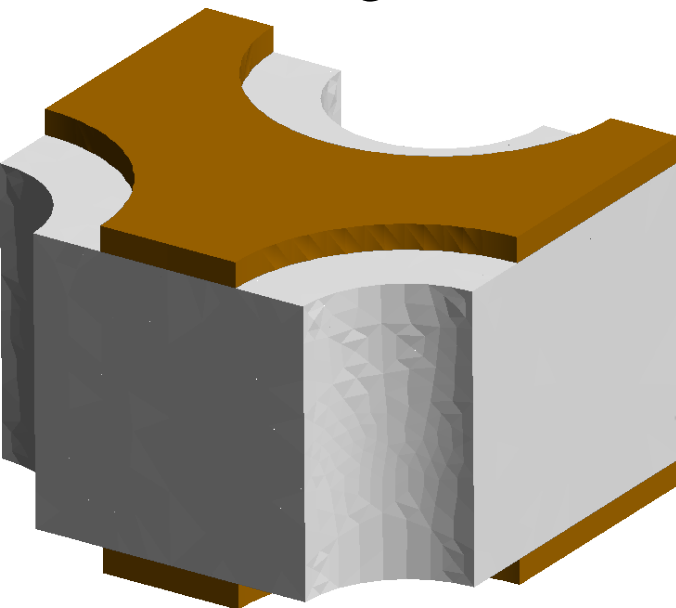
- ▶ Finite element programs are nearly always commercial.
- ▶ A rare exception is Gmsh/Elmer. Josh Renner (Berkeley) has written a Garfield++ interface.

C. Geuzaine and J.-F. Remacle, *Gmsh: a three-dimensional finite element mesh generator with built-in pre- and post-processing facilities*, <http://geuz.org/gmsh/>.

CSC – IT Center for Science, *Elmer: Open Source Finite Element Software for Multiphysical Problems*, <http://www.csc.fi/english/pages/elmer>.

Gmsh/Elmer example

- ▶ Thick GEM
- ▶ unit cell,
- ▶ avalanche,
- ▶ signal.



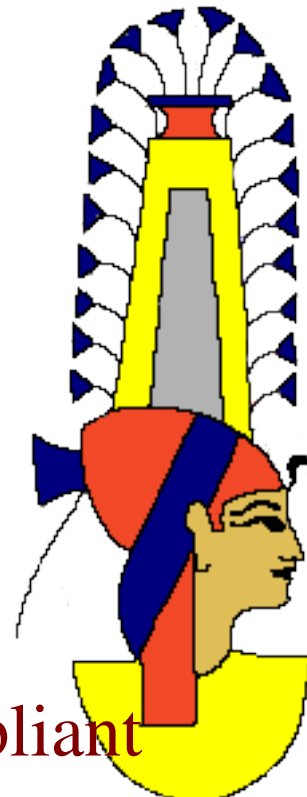
Josh Renner: <http://cern.ch/garfieldpp/examples/elmer/>

The price to pay for finite elements

- ▶ Finite elements focus (for us) on the wrong thing:
 - ▶ they solve V well, but we do not really need it:
 - ▶ Quadratic shape functions can do a fair job at approximating $V \approx \log(r)$ potentials.
 - ▶ Potentials are continuous.
 - ▶ E is what we use, but:
 - ▶ Gradients of quadratic shape functions are linear *i.e.* unsuitable to approximate our $E \approx 1/r$ fields with, left alone $E \approx 1/r^2$ fields.
 - ▶ Electric fields are discontinuous.
 - ▶ A local accuracy of ~50 % in high-field areas is not unheard of.
- ▶ In exchange, we get a lot of flexibility.

Boundary element methods

- ▶ Contrary to the finite element method, the elements are on the boundaries, not in the problem domain. Charges are computed for the boundary elements.
- ▶ The field is calculated as the sum of **Maxwell-compliant field functions**, each extending over the entire problem domain. There are **no discontinuities**.
- ▶ In contrast, the method poses substantial numerical challenges: non-sparse matrices and inherent singularities.
- ▶ neBEM has explicit Green's functions for uniformly charged triangles and rectangles.



$$\Phi = \frac{1}{2} ((z_M Y^2 - XG)(LP_1 + LM_1 - LP_2 - LM_2) + i|Y|(z_M X + G)(LP_1 - LM_1 - LP_2 + LM_2) - S_1 X (\tanh^{-1}(\frac{R_1 + iI_1}{D_{11}|Z|}) + \tanh^{-1}(\frac{R_1 - iI_1}{D_{11}|Z|}) - \tanh^{-1}(\frac{R_1 + iI_2}{D_{21}|Z|}) - \tanh^{-1}(\frac{R_1 - iI_2}{D_{21}|Z|})) - iS_1 |Y| (\tanh^{-1}(\frac{R_1 + iI_1}{D_{11}|Z|}) - \tanh^{-1}(\frac{R_1 - iI_1}{D_{11}|Z|}) - \tanh^{-1}(\frac{R_1 + iI_2}{D_{21}|Z|}) + \tanh^{-1}(\frac{R_1 - iI_2}{D_{21}|Z|})) + \frac{2G}{\sqrt{1+z_M^2}} \log(\frac{\sqrt{1+z_M^2}D_{12} - E_1}{\sqrt{1+z_M^2}D_{21} - E_2}) + 2Z \log\left(\frac{D_{21} - X + 1}{D_{11} - X}\right) + C$$

- For computing the field at any point, neBEM sums the fields due to each element on that point.

$$D_{11} = \sqrt{(X - x_1)^2 + Y^2 + (Z - z_1)^2}; D_{12} = \sqrt{(X - x_1)^2 + Y^2 + (Z - z_2)^2}$$

$$D_{21} = \sqrt{(X - x_2)^2 + Y^2 + (Z - z_1)^2}; I_1 = (X - x_1) |Y|; I_2 = (X - x_2) |Y|$$

$$S_1 = \text{sign}(z_1 - Z); R_1 = Y^2 + (Z - z_1)^2$$

- Evaluating the Green's functions, especially the one for triangular elements, is costly.

$$LP_1 = \frac{1}{G - iz_M|Y|} \log\left(\frac{(H_1 + GD_{12}) + i|Y|(E_1 - iz_M D_{12})}{-X + i|Y|}\right)$$

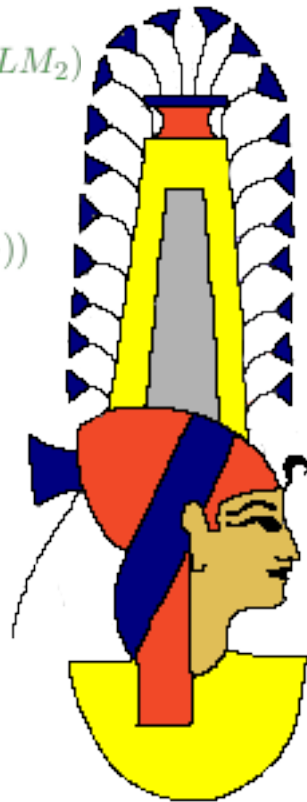
- For a modest doubly-periodic 1000-element model there would be $\sim 10^8$ function evaluations. For an avalanche study we would love to have 1000. We then need to compute the field at $\sim 10^7$ points.

$$LM_1 = \frac{1}{G + iz_M|Y|} \log\left(\frac{(H_1 + GD_{12}) + i|Y|(E_1 - iz_M D_{12})}{-X - i|Y|}\right)$$

$$LP_2 = \frac{1}{G - iz_M|Y|} \log\left(\frac{(H_2 + GD_{21}) + i|Y|(E_2 - iz_M D_{21})}{-X + i|Y|}\right)$$

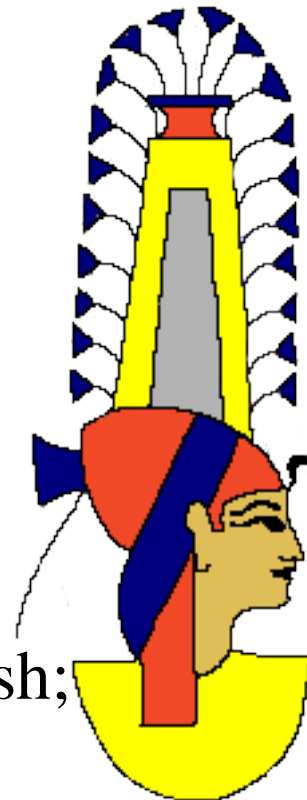
$$LM_2 = \frac{1}{G + iz_M|Y|} \log\left(\frac{(H_2 + GD_{21}) + i|Y|(E_2 - iz_M D_{21})}{1 - X - i|Y|}\right)$$

and C denotes a constant of integration.



Towards a faster neBEM

- ▶ Optimisation has made the program 75 % faster.
- ▶ Next step is the introduction of a “fast volume”:
 - ▶ in the fast volume the field is pre-computed on a mesh;
 - ▶ inside, the field is interpolated (finite element style);
 - ▶ outside, the field is computed as is done now.



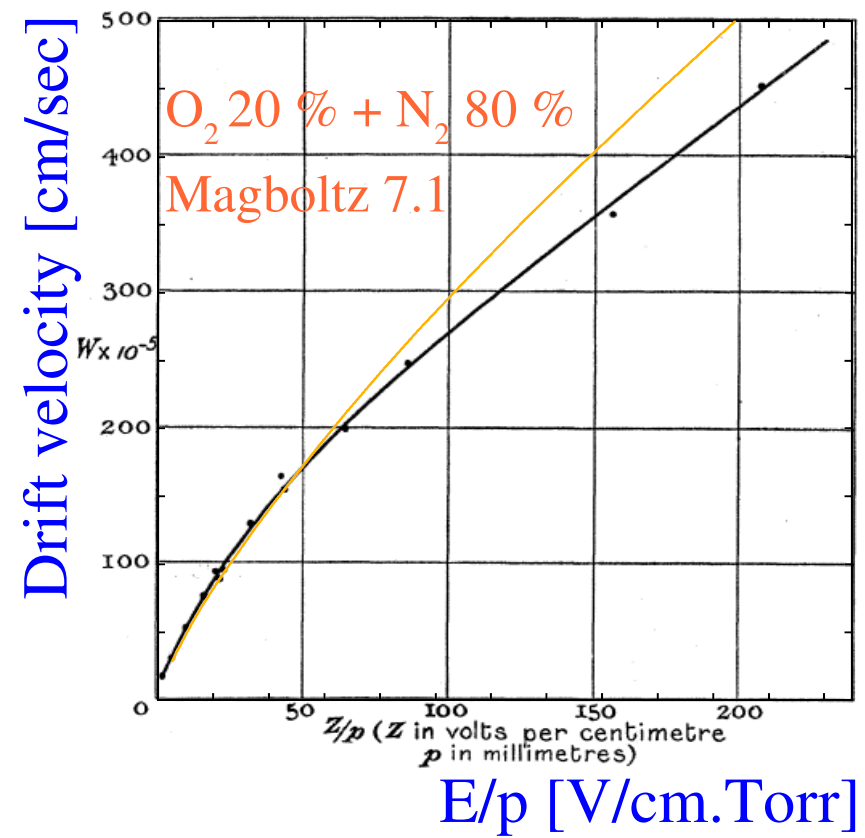
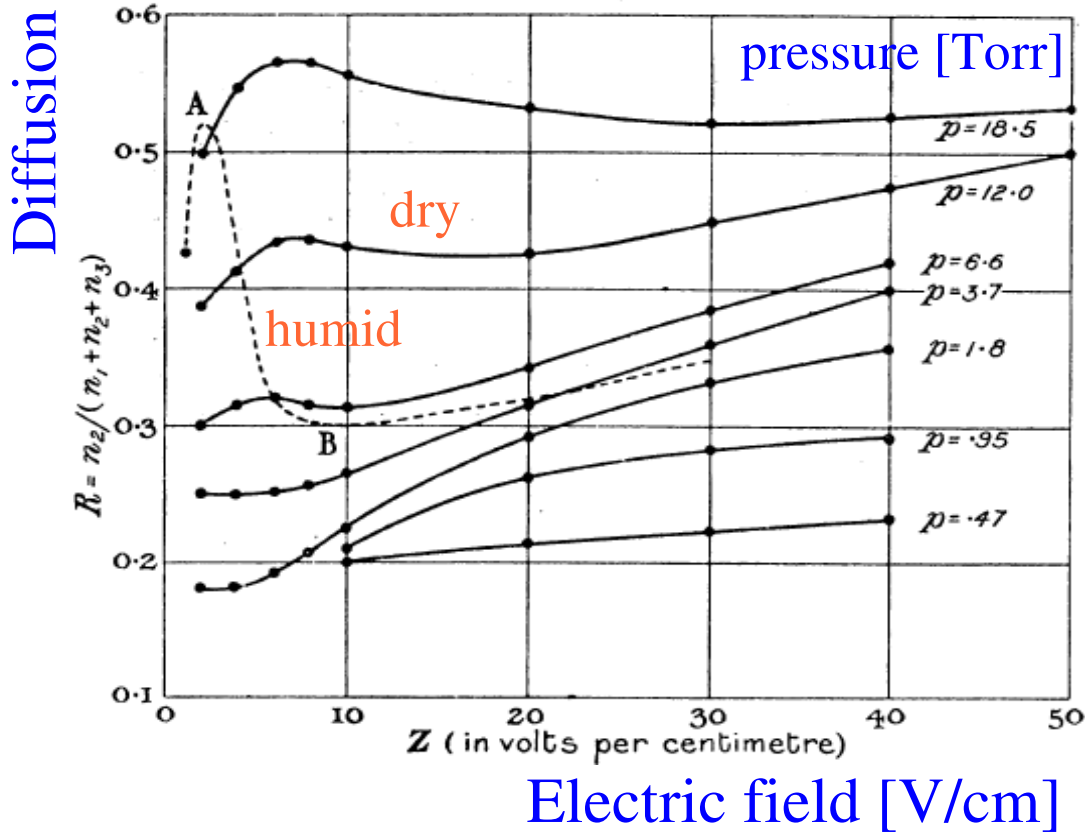
Drift field (V/cm)	Transparency Exact computation	Transparency Fast algorithm	Gain (RKF) Exact Computation	Gain (RKF) Fast algorithm
200	99.835	99.864	250.133	250.139
400	99.669	99.471		
750	96.364	95.774		
1500	70.248	71.214		
2000	59.669	58.791		
	Time taken for 500 electrons ~150 hours	Time taken for 20,000 electrons ~ 25 hours	Time ~ 40 minutes	Time ~ less than a minute

1900: Electron transport in gases

- ▶ The velocity of positive and negative “ions” produced in gases by Röntgen rays was extensively studied at the turn of the century, as shown by the abundant literature, *e.g.*
 - ▶ E. Rutherford, Phil. Mag. **44** (1897) 422;
 - ▶ J. Zeleny, Phil. Trans. R. Soc. Lond. A **195** (1900) 193-234;
 - ▶ J.S. Townsend, Nature **62** (1900) 340-341;
 - ▶ J.S. Townsend, Phil. Mag. **6-1** (1901) 198-227.
- ▶ Drift velocities, diffusion coefficients and Townsend coefficients were measured and interpreted.

Measurements of velocity and diffusion

► Examples of measurements in air from 1913:



J. S. Townsend and H. T. Tizard, *The Motion of Electrons in Gases*,
Proc. R. Soc. Lond. A 88 (1913) 336-347.



1962: Numerical e⁻ transport

- ▶ Iterative approach, allowing for inelastic cross section terms:
 - ▶ educated guess of cross sections (elastic & inelastic);
 - ▶ numerically solve the Boltzmann equation (no moments);
 - ▶ compare calculated and measured mobility and diffusion;
 - ▶ adjust cross sections.

“... more than 50,000 transistors plus extremely fast magnetic core storage. The new system can simultaneously read and write electronically at the rate of 3,000,000 bits of information a second, when eight data channels are in use. In 2.18 millionths of a second, it can locate and make ready for use any of 32,768 data or instruction numbers (each of 10 digits) in the magnetic core storage. The 7090 can perform any of the following operations in one second: 229,000 additions or subtractions, 39,500 multiplications, or 32,700 divisions. “ (IBM 7090 documentation)

[L.S. Frost and A.V. Phelps, *Rotational Excitation and Momentum Transfer Cross Sections for Electrons in H₂ and N₂ from Transport Coefficients*, Phys. Rev. **127** (1962) 1621–1633.]

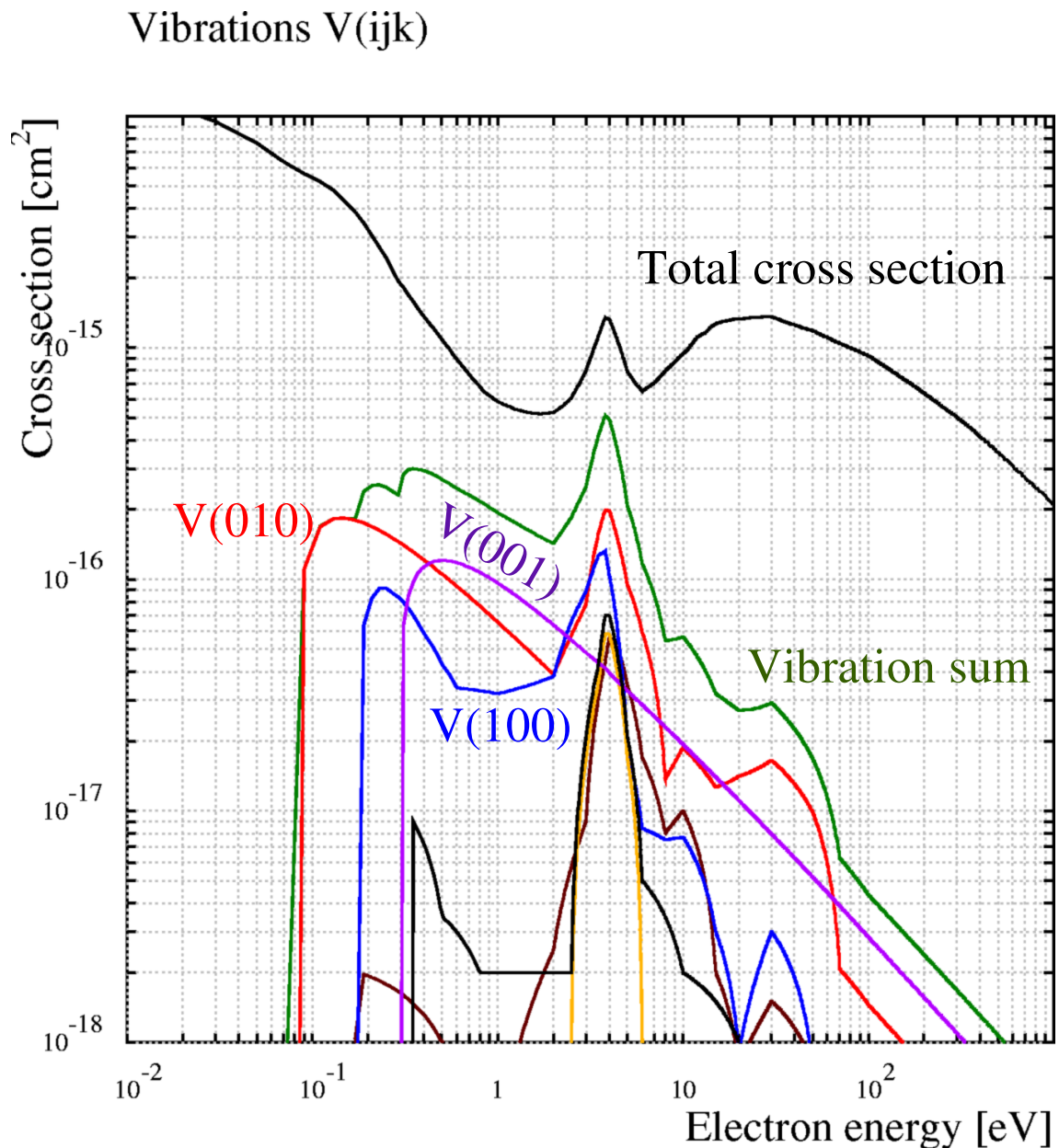
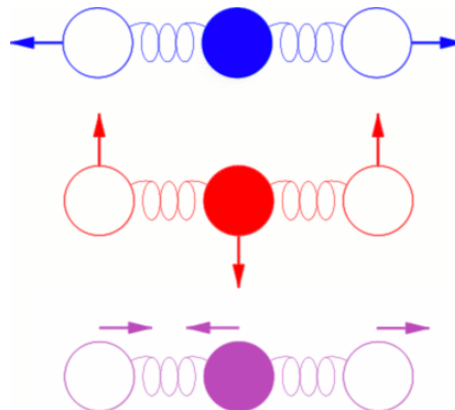


2000: Magboltz MC – Steve Biagi

- ▶ A large number of cross sections for 60 molecules...
 - ▶ All noble gases, *e.g.* argon:
 - ▶ elastic scattering,
 - ▶ 44 excited states and
 - ▶ ionisation.
 - ▶ Numerous organic gases, additives, *e.g.* CO₂:
 - ▶ elastic scattering,
 - ▶ 44 inelastic cross sections (vibrations, rotations, polyads)
 - ▶ 35 super-elastic cross sections,
 - ▶ 6 excited states,
 - ▶ attachment and
 - ▶ ionisation.

CO_2 – vibration modes

- ▶ CO_2 is linear:
- ▶ O – C – O
- ▶ Vibration modes are numbered $V(ijk)$
 - ▶ i : symmetric,
 - ▶ j : bending,
 - ▶ k : anti-symmetric.



1e-18

LXcat, <http://www.lxcat.laplace.univ-tlse.fr>
Generated on 21 Jan 2011. All rights reserved.

Argon cross section terms

Elastic

Ionisation

Cross section, m²

- ELASTIC_Ar (Biagi-v8.9) —— red
- Ar → Ar(1S5)(11.55eV) —— green
- Ar → Ar(1S4)(11.62eV) —— blue
- Ar → Ar(1S3)(11.72eV) —— magenta
- Ar → Ar(1S2)(11.83eV) —— cyan
- Ar → Ar(2P10)(12.91eV) —— brown
- Ar → Ar(1P9)(13.08eV) —— yellow
- Ar → Ar(2P8)(13.10eV) —— dark blue
- Ar → Ar(2P7)(13.15eV) —— orange
- Ar → Ar(2P6)(13.17eV) —— dark green
- Ar → Ar(2P5)(13.27eV) —— purple
- Ar → Ar(2P4)(13.28eV) —— brown
- Ar → Ar(2P3)(13.30eV) —— pink
- Ar → Ar(2P2)(13.33eV) —— light green
- Ar → Ar(2P1)(13.48eV) —— cyan
- Ar → Ar(3D6)(13.85eV) —— dark blue
- Ar → Ar(2D5)(13.86eV) —— pink
- Ar → Ar(3D3)(13.90eV) —— dark green
- Ar → Ar(3D4)(13.98eV) —— light green
- Ar → Ar(3D4)(14.01eV) —— dark blue
- Ar → Ar(3D1!!)(14.06eV) —— brown
- Ar → Ar(2S5)(14.07eV) —— grey
- Ar → Ar(2S4)(14.09) —— green
- Ar → Ar(3D1!)(14.10eV) —— dark blue
- Ar → Ar(3D2)(14.15eV) —— brown
- Ar → Ar(3S1!!!!)(14.21eV) —— grey
- Ar → Ar(3S1!!!)(14.23eV) —— grey
- Ar → Ar(3S1!!!)(14.24eV) —— dark blue
- Ar → Ar(2S3)(14.24eV) —— blue
- Ar → Ar(2S2)(14.25eV) —— dark green
- Ar → Ar(3S1)(14.30eV) —— pink
- Ar → Ar(4D5)(14.71eV) —— light green
- Ar → Ar(3S4)(14.85eV) —— dark blue
- Ar → Ar(4D2)(14.86eV) —— brown
- Ar → Ar(4S1!)(15.00eV) —— light green
- Ar → Ar(3S2)(15.02eV) —— brown
- Ar → Ar(5D5)(15.12eV) —— magenta
- Ar → Ar(4S4)(15.19eV) —— purple
- Ar → Ar(5D2)(15.19eV) —— grey
- Ar → Ar(6D5)(15.31eV) —— grey
- Ar → Ar(5S1!)(15.35eV) —— grey
- Ar → Ar(4S2)(15.36eV) —— blue
- Ar → Ar(5S4)(15.37eV) —— brown
- Ar → Ar(6D2)(15.37eV) —— grey
- Ar → Ar(EXC HIGH)(15.66eV) —— light green
- Ar → Ar⁺ —— olive

0.001

0.01

0.1

1

10

100

1000

Energy, eV

LXcat

- ▶ Art Phelps,
- ▶ Leanne Pitchford – Toulouse,
- ▶ Klaus Bartschat – Iowa,
- ▶ Oleg Zatsarinny – Iowa,
- ▶ Michael Allan – Fribourg,
- ▶ Steve Biagi

Leanne Pitchford



Michael Allan



Klaus Bartschat



LXcat (pronounced *elecscat*) is an open-access website for collecting, displaying, and downloading ELECtron SCATtering cross sections and swarm parameters (mobility, diffusion coefficient, reaction rates etc.) required for modeling low temperature plasmas. [...]”

<http://www.lxcat.laplace.univ-tlse.fr/>

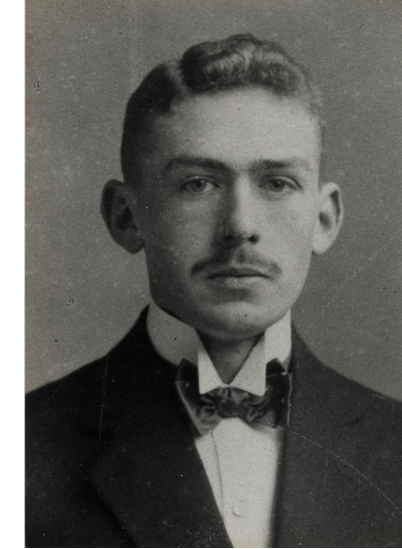


1901: Gas multiplication

- ▶ John Townsend “*The conductivity produced in gases by the motion of negatively charged ions*”:

Negative Ionen erzeugen bei ihrer Wanderung durch Berührung neue Ionen. Die Anzahl der negativen Ionen in einer Entfernung x vom Punkte der Entstehung ist deshalb durch die Exponentialfunktion in der Form $N = N_0 e^{\alpha x}$ gegeben. Diese Formel wird durch Versuche bestätigt. Dabei ist α eine Größe, die außer von der Temperatur noch von der Größe der die Ionen bewegenden Kraft X und dem Druck p abhängt, und zwar ergibt sich diese Abhängigkeit in der Form $= p f(X/p)$.

Frans Michel Penning,
photo taken around 1921
(1894-1953)



1928: Ar-Ne-Hg Penning effects

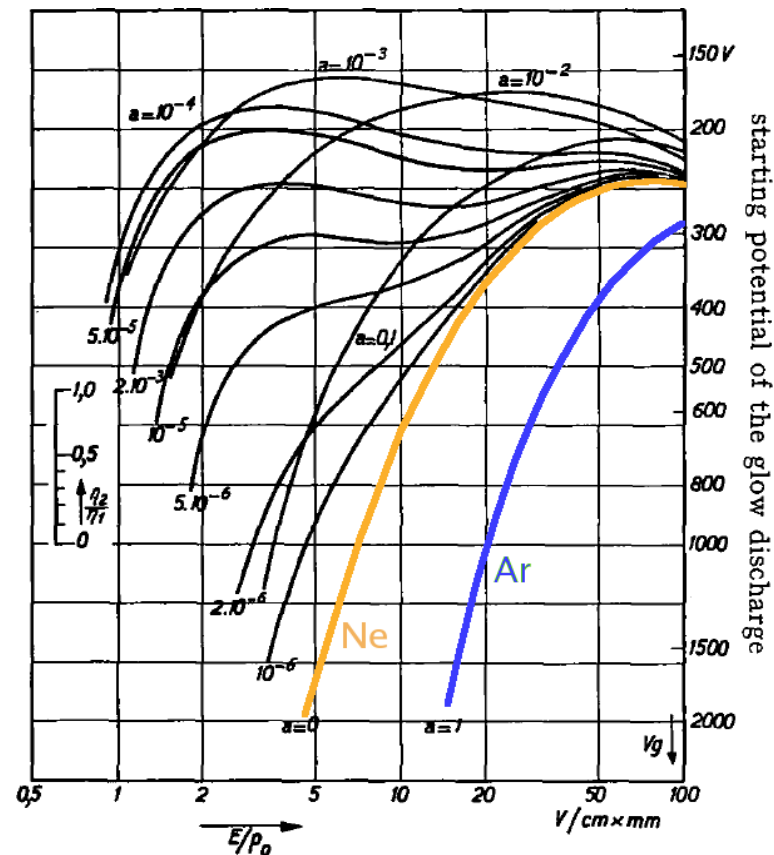
► Frans Michel Penning worked from 1924 on gas discharges at the Philips Natuurkundig Laboratorium.

Der Einfluß sehr geringer Beimischung von Hg und Ar auf die Zündspannung V_z des Neons wurde quantitativ bestimmt. Die Erklärung wurde gefunden in der Ionisierung der Fremdatome durch die metastabilen Atome des Neons. Die notwendige Bedingung für diesen Vorgang: $V'_i < V_{\text{met.}}$ wurde geprüft bei Ne, Ar und He als Hauptgasen mit verschiedenen anderen Gasen als Beimischung und stets bestätigt gefunden. Andererseits erniedrigten immer Beimischungen, wobei $V'_i < V_{\text{met.}}$ die Zündspannung; nur NO in Ar machte eine Ausnahme von dieser Regel, was aber auf Grund des Termschemas von NO nicht zu verwundern braucht.

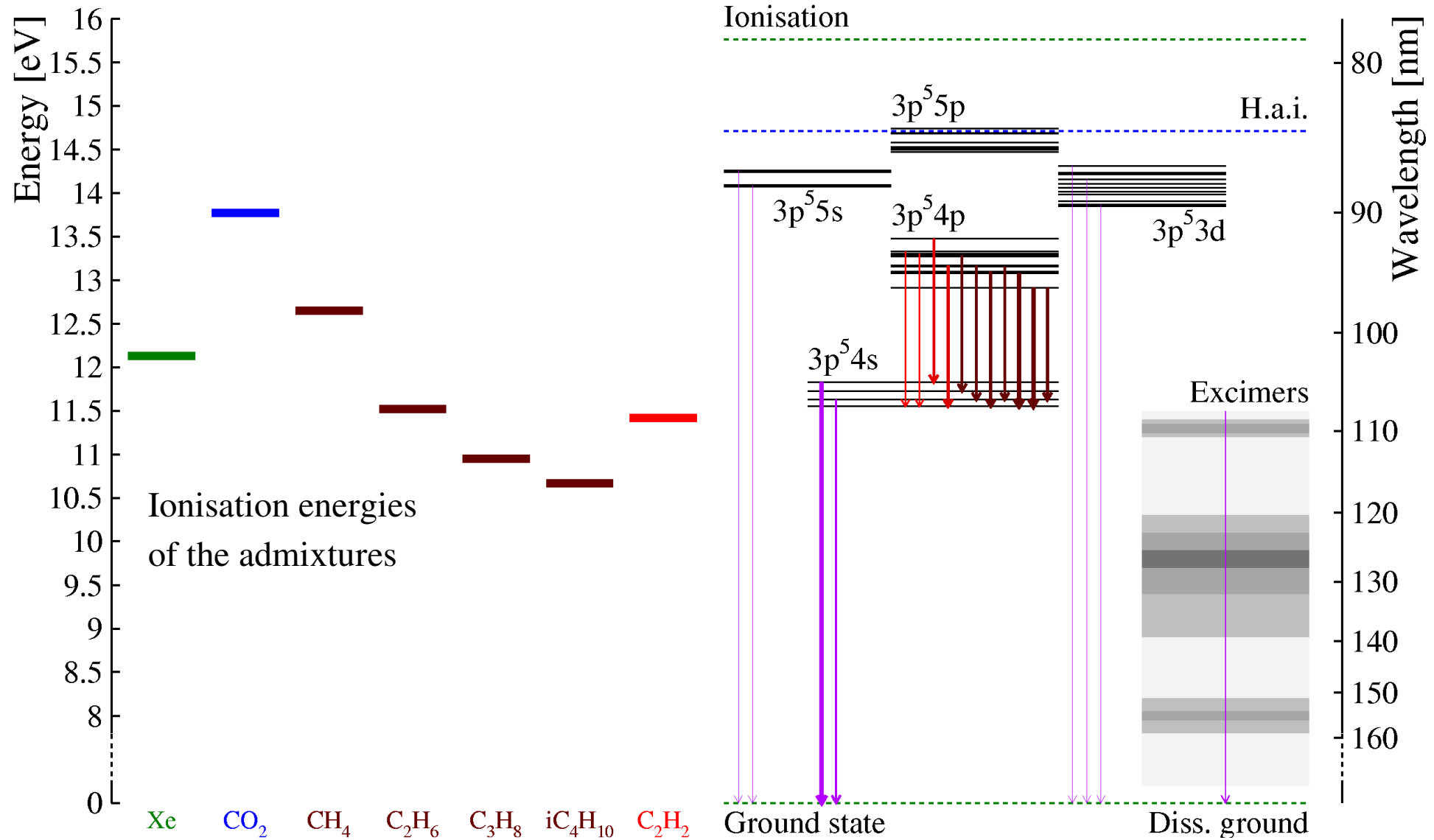
F. M. Penning, *Über den Einfluß sehr geringer Beimischungen auf die Zündspannung der Edelgase*, Z. Phys. **46** (1928) 334-348.

F.M. Penning, *The starting potential of the glow discharge in neon argon mixtures between large parallel plates: II. Discussion of the ionisation and excitation by electrons and metastable atoms*, Physica **1** (1934) 1028-1044.

F.M. Penning, *Electrische gasontladingen*, Philips Technische Bibliotheek (posthumous, 1955). Translated in various languages.



Level diagram argon and admixtures

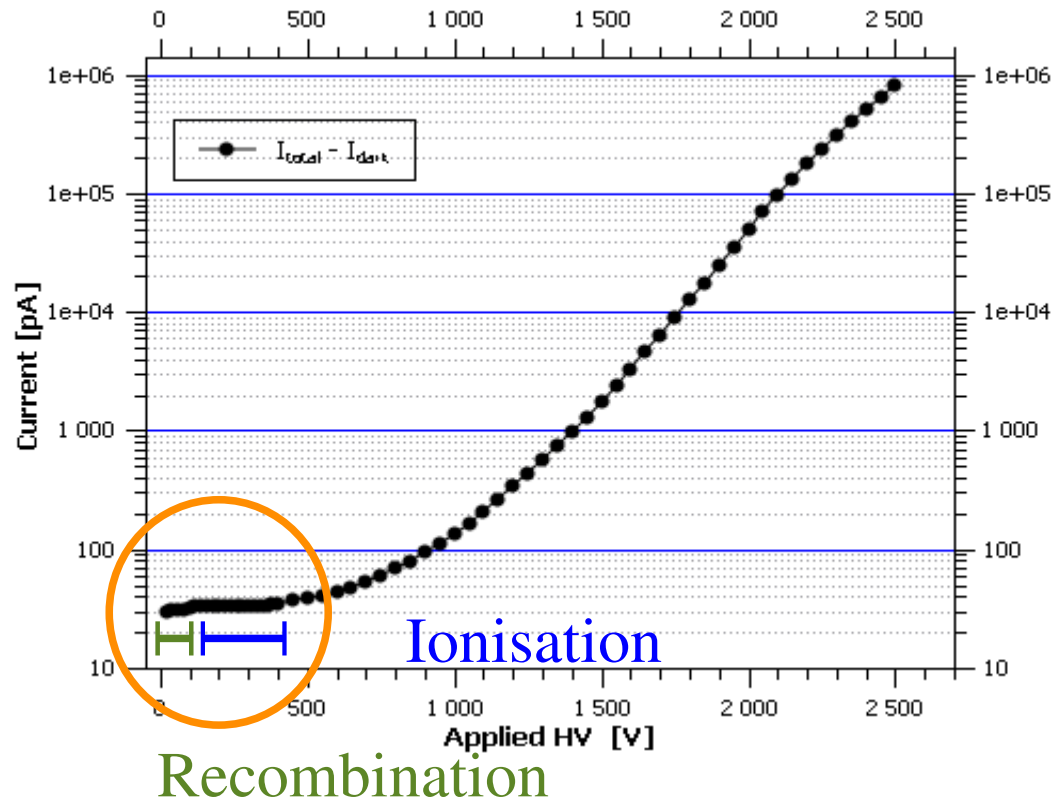
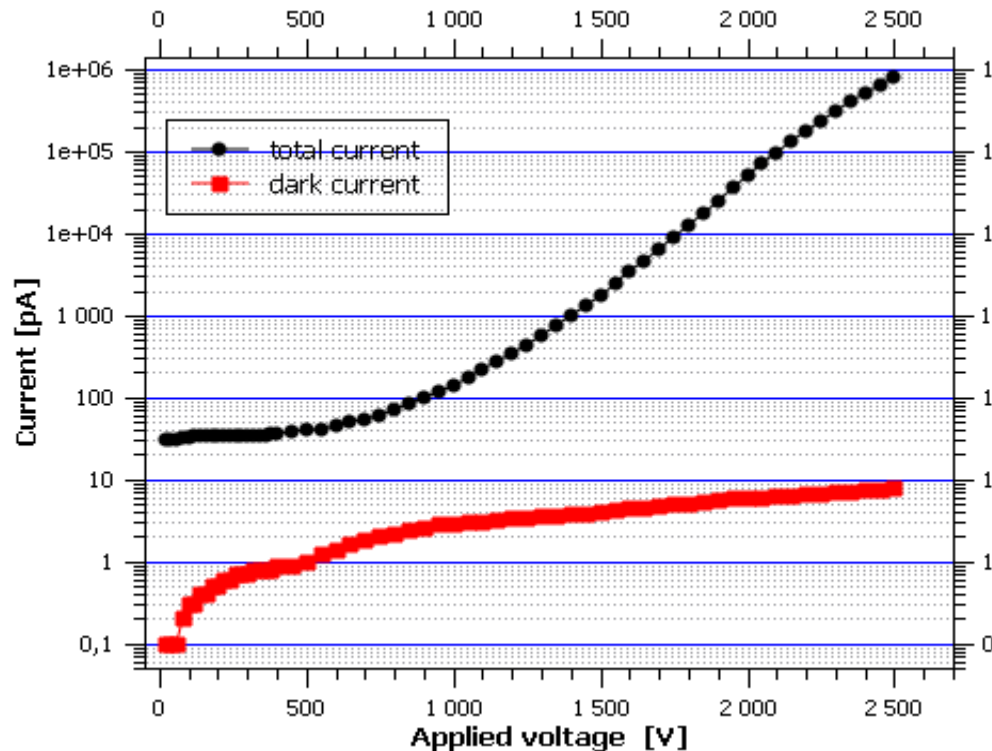


Excitation energy transfer

- ▶ Noble gas A^* is excited and admixture B is ionised:
 - ▶ dipole-dipole coupling: $A^* \rightarrow A \gamma, \gamma B \rightarrow B^+ e^-$
 - ▶ e^- exchange (“Auger”): $A^* B \rightarrow A^{*-} B^+, A^{*-} \rightarrow A e^-$
 - ▶ associative ionisation: $A^* A \rightarrow A_{_2}^+ e^-$
 - ▶ excimers in some gases.
- ▶ A^* decay can give γ 's which ionise or cause feedback, a domain increasingly regaining prominence.
- ▶ Partial pressure dependence differs for 1-, 2- and 3-body.
- ▶ Few rate constants are known: need for experimental data.

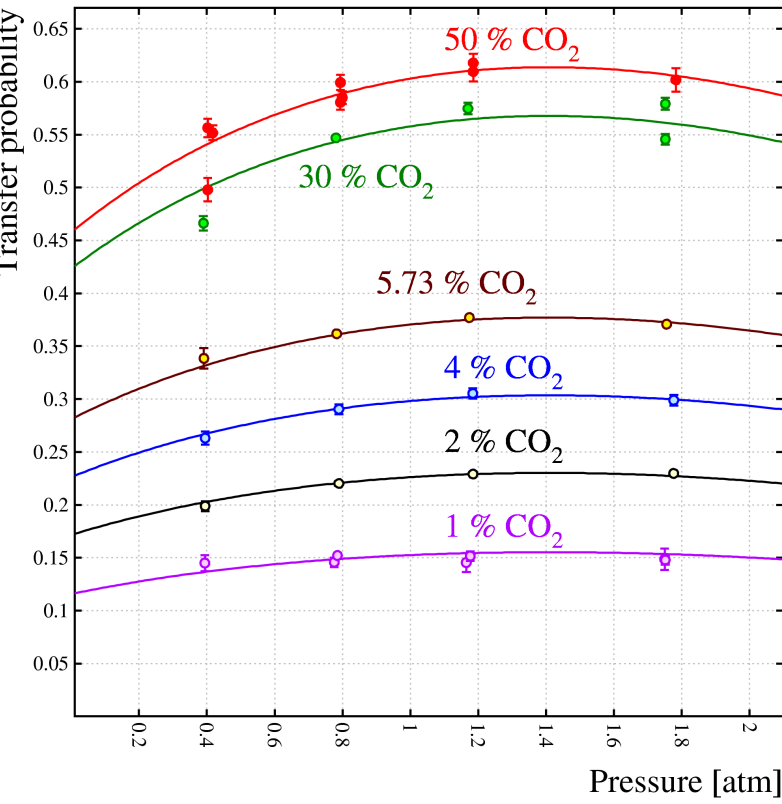
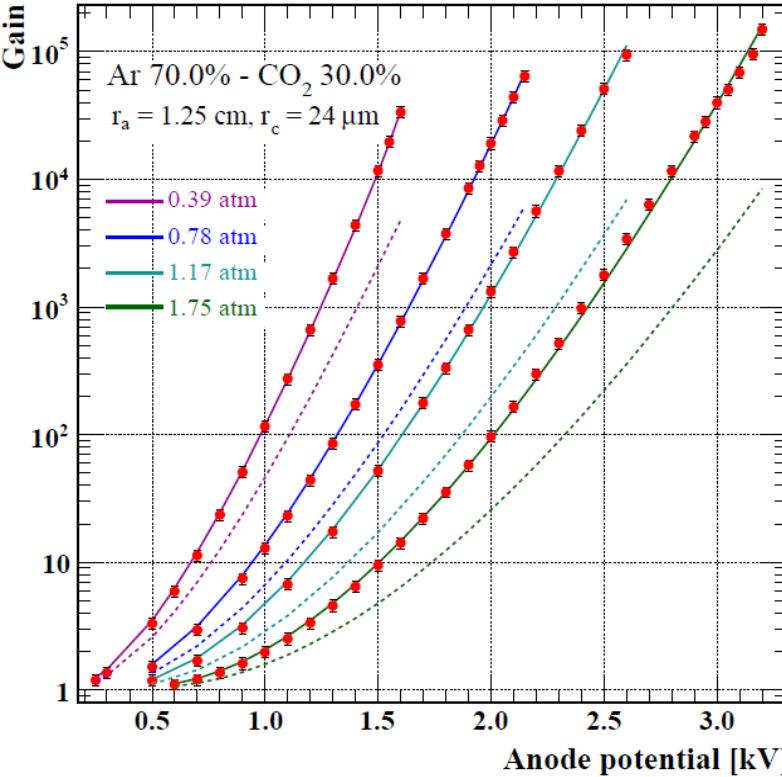
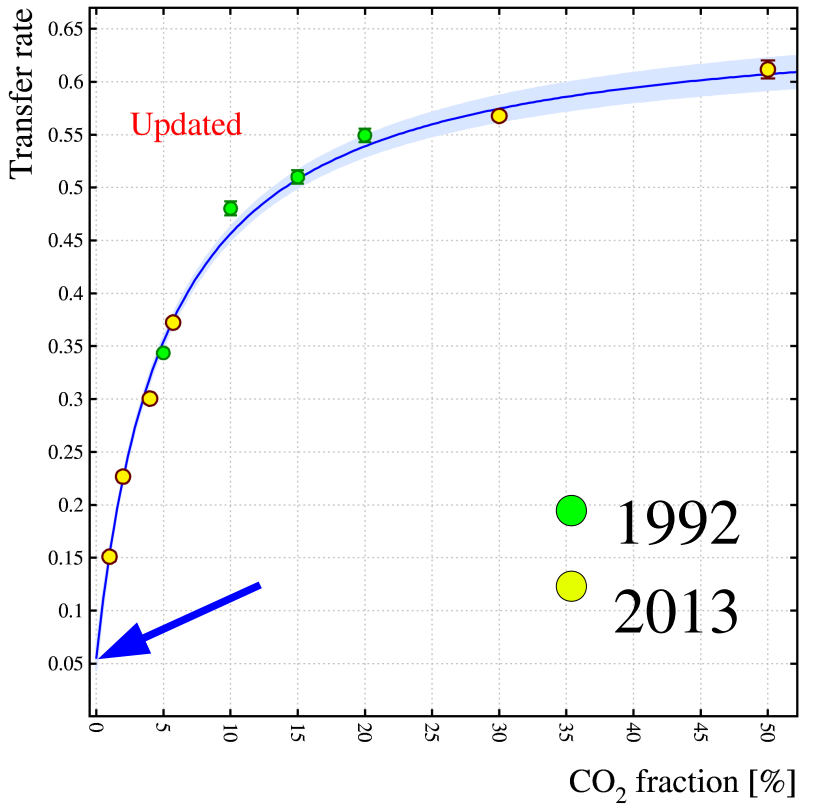
Example of measurements

- ▶ Ar-CO₂-N₂ [91.1-6.4- 2.5] at $p = 0.2 \text{ MPa}$;
- ▶ dark current measurement and subtraction:



Ar-CO₂

- Radiative term physical and rise of r_p saturates, as seen in GEMs.
- Measurements: Tadeusz Kowalski et al. AGH Kraków. Fits: Özkan Şahin, Uludağ. See their presentation.



Paul Langevin
(1872-1946)



1905 – Paul Langevin: ion mobility

- ▶ Expression for the mobility when interactions between the ion and induced molecular dipoles dominate:

Ce cas extrême correspond à une influence négligeable des chocs élastiques, c'est-à-dire au déplacement dans un gaz d'une particule électrisée de dimensions extrêmement petites, dont le déplacement à l'intérieur du gaz est généralement principalement par son attraction pour les molécules.

On aurait, pour la mobilité correspondante,

$$k_0 = \frac{0,505}{\sqrt{(K-1)\rho}} \sqrt{\frac{m+m_1}{m_1}}.$$

K = pouvoir inducteur spécifique

m, m_1 = mass of molecule and ion

Ions attracting polarisable gas molecules

- ▶ Calculation of the force exercised by a charge on surrounding molecules.
($M = n$, number density)

calculons le moment électrostatique μ de la molécule d'oxygène polarisée par un champ électrique X . Si K' est le pouvoir inducteur spécifique du gaz, le moment électrique de l'unité de volume est égal à la polarisation

$$A = \frac{(K' - 1)X}{4\pi}.$$

Et si M est le nombre des molécules par unité de volume,

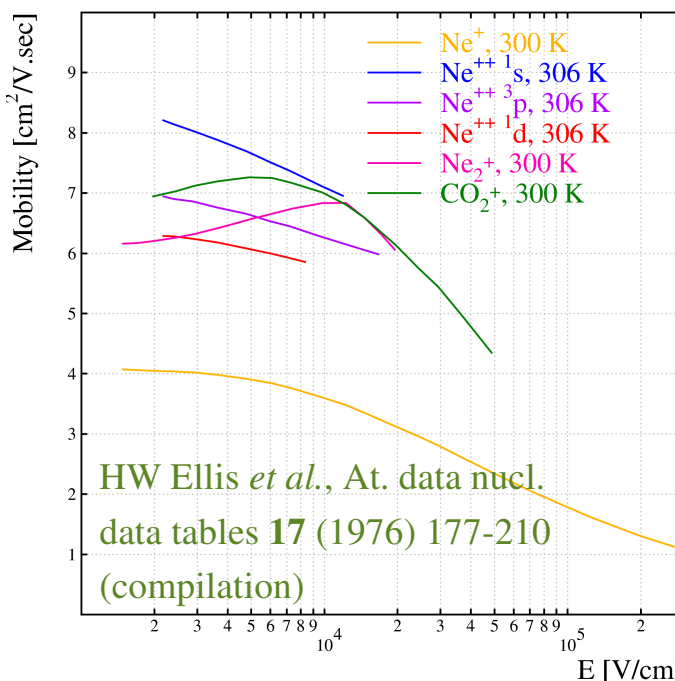
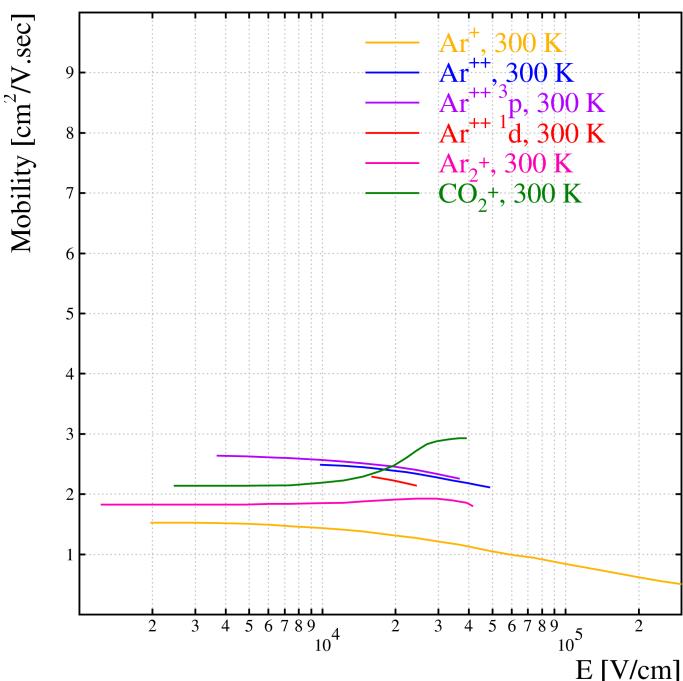
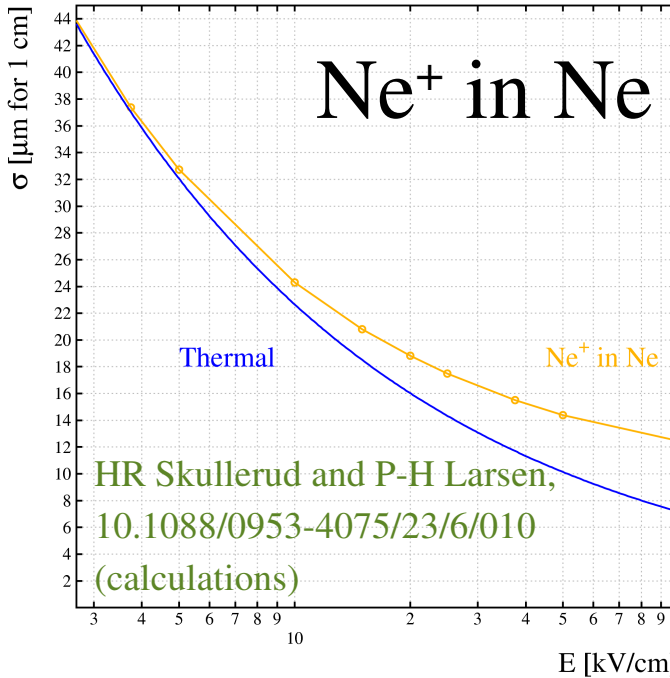
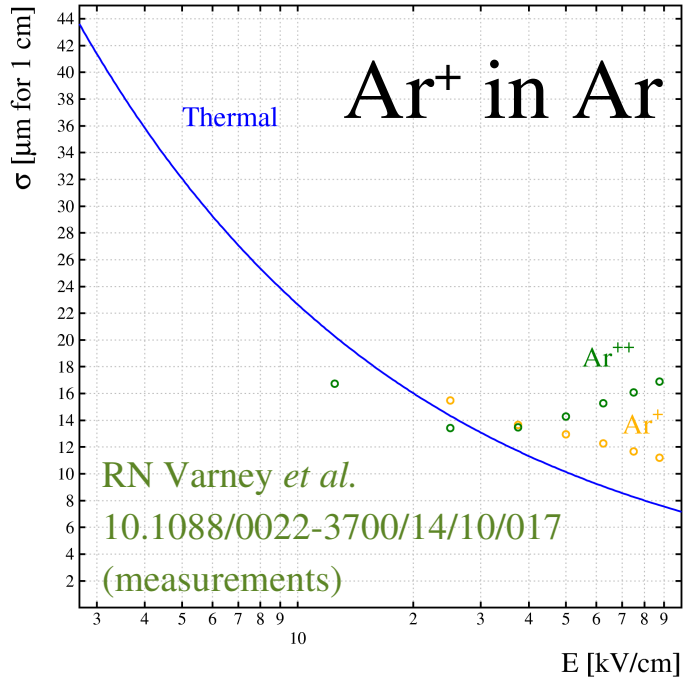
$$\mu = \frac{A}{M} = \frac{(K' - 1)X}{4\pi M}.$$

L'ion qui porte une charge $e' = 7 \times 10^{-10}$ produit à la distance r un champ $\frac{e'}{r^2}$, et la force attractive qui en résulte sur la molécule est

$$f = \mu \frac{dX}{dr} = \frac{K' - 1}{4\pi M} X \frac{dX}{dr} = \frac{K' - 1}{2\pi M} \frac{e'^2}{r^5} (1).$$

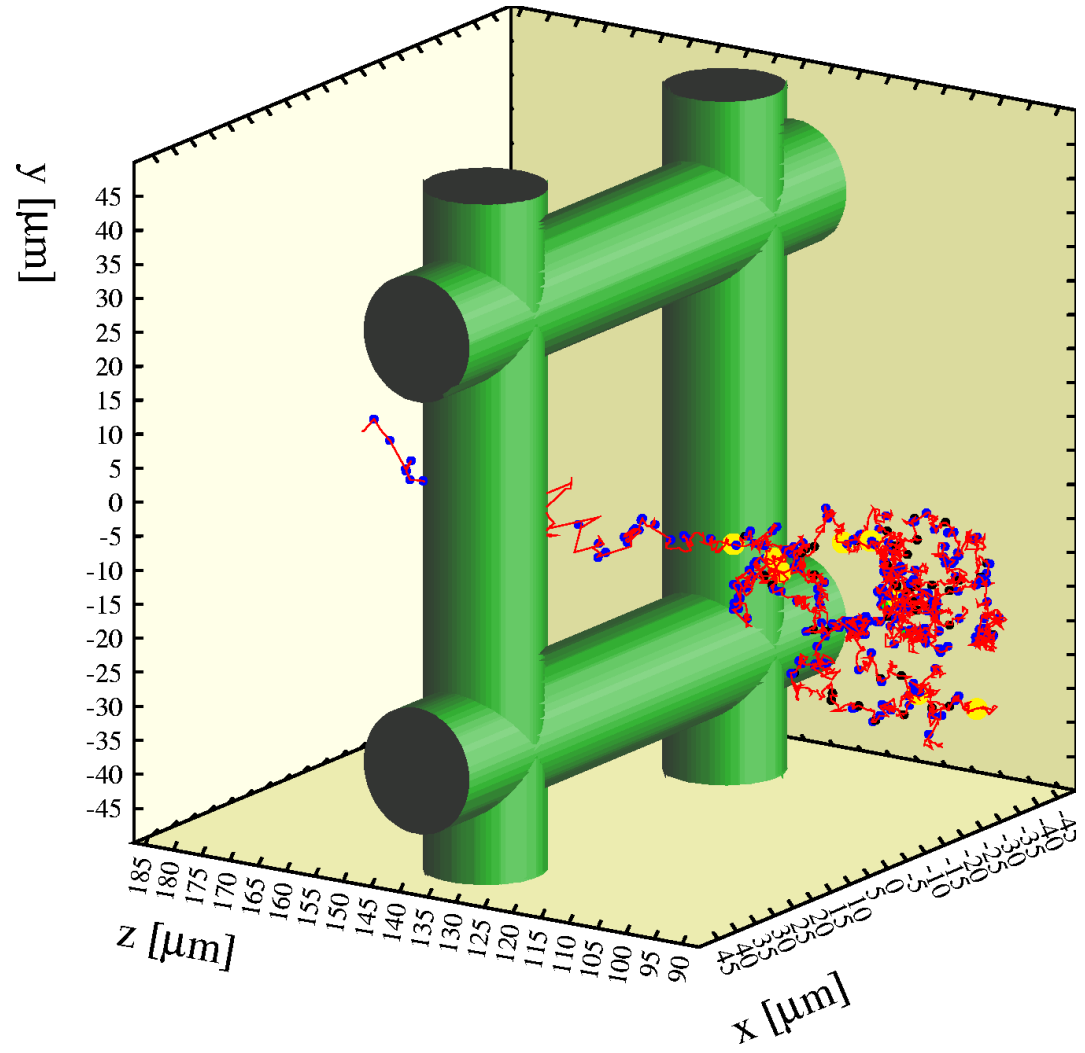
The force decays $\sim 1/r^5$.

Ion mobility and diffusion – data



See presentation
by André Cortez

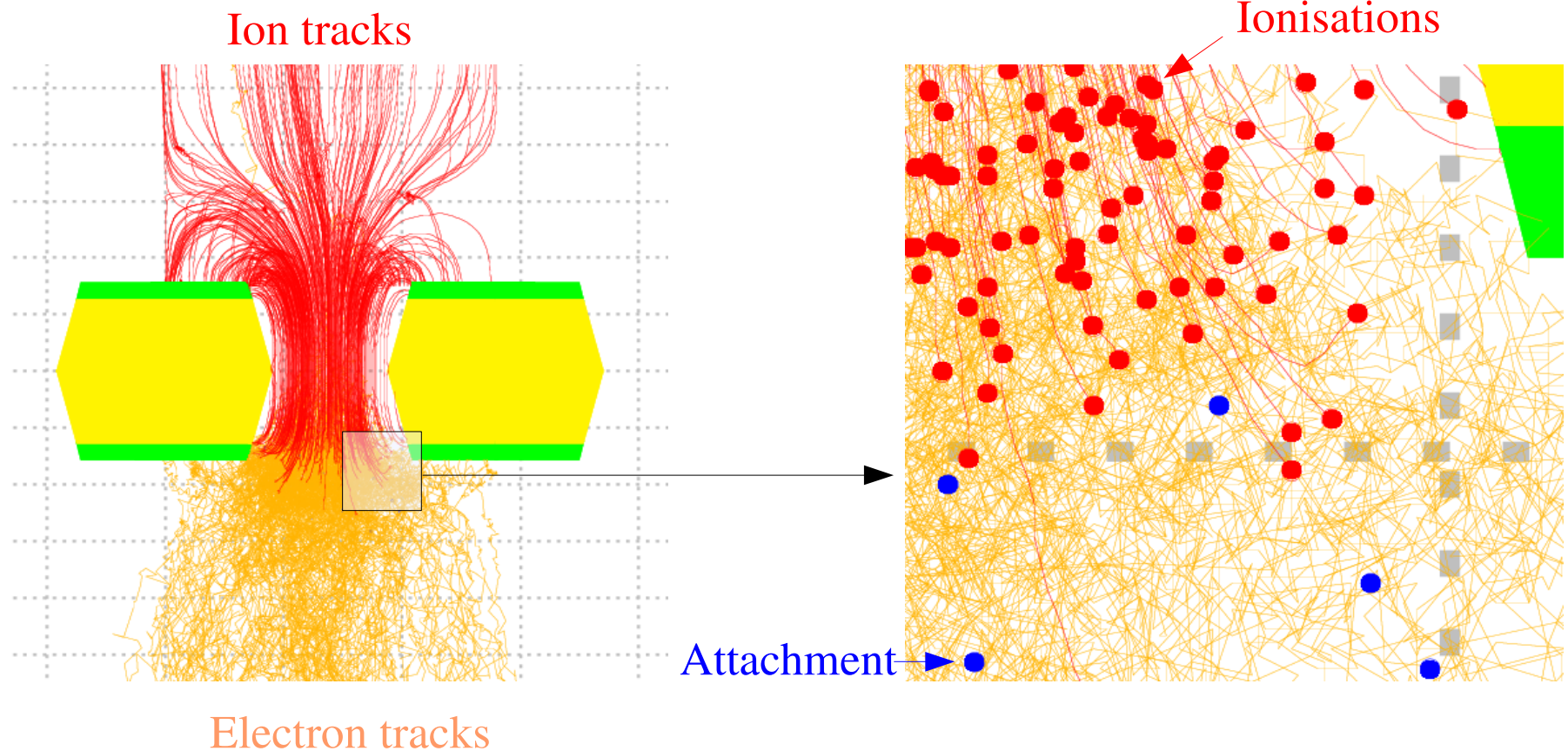
Microscopic Micromegas



- ▶ Legend:
 - ▶ – electron
 - ▶ ○ inelastic
 - ▶ ● excitation
 - ▶ ○ ionisation

Electron tracking at molecular level

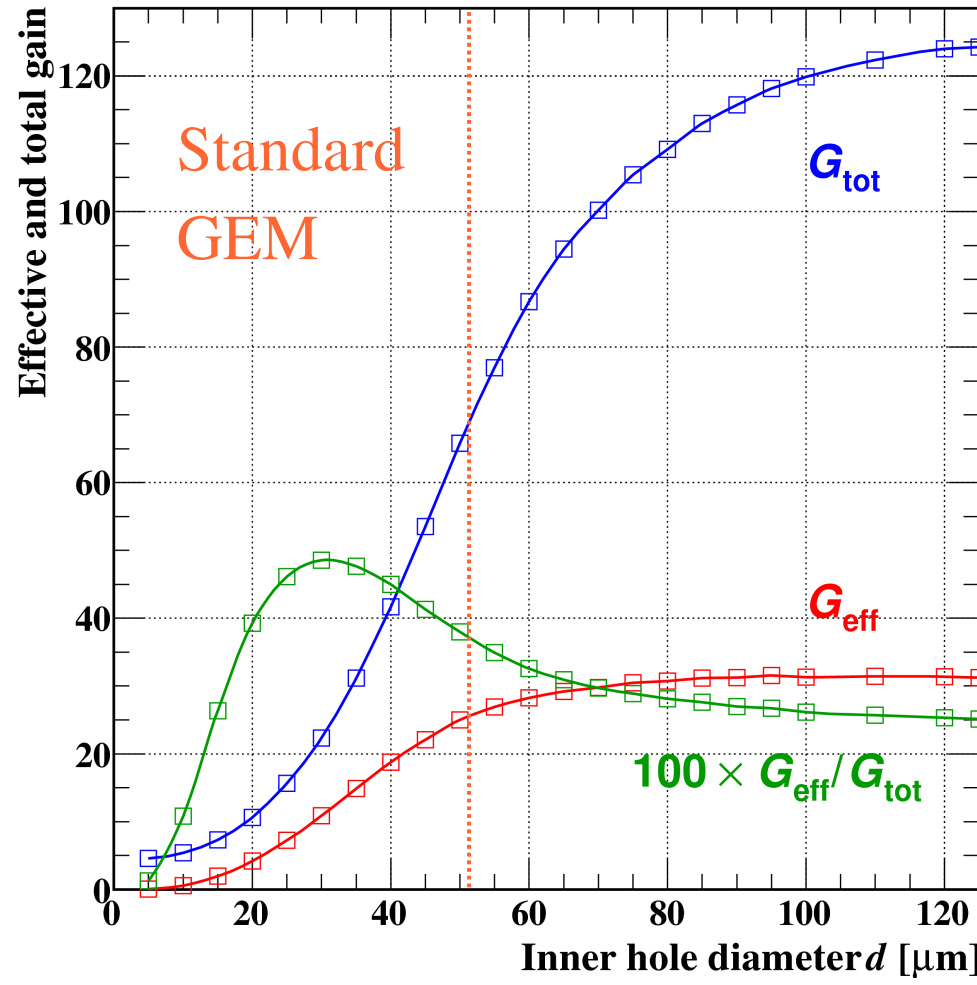
- ▶ Micropattern devices have characteristic dimensions that are comparable with the mean free path.



[Plot by Gabriele Croci and Matteo Alfonsi]

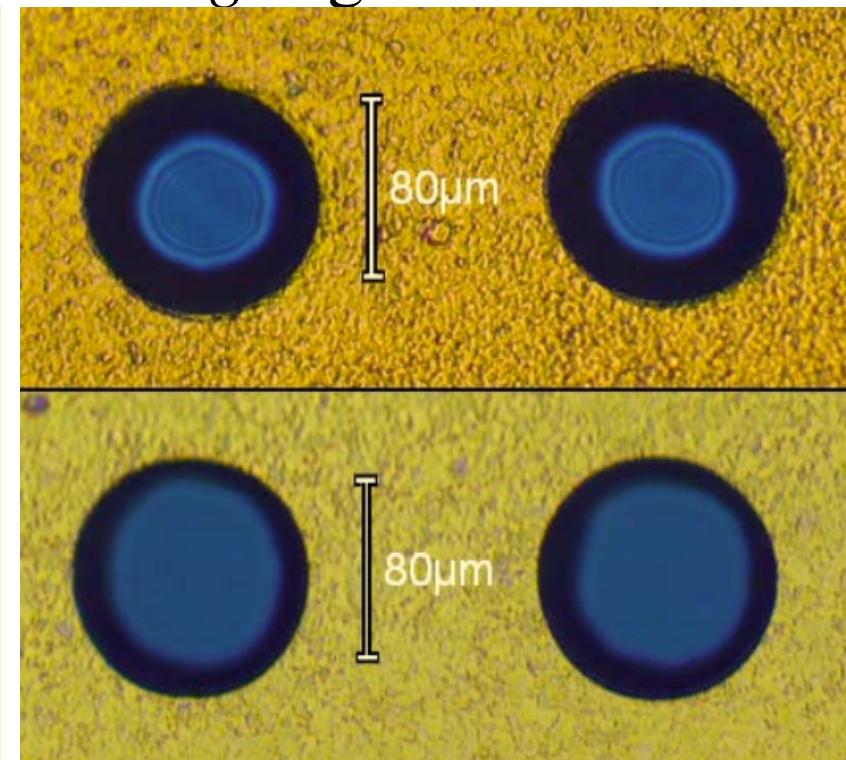
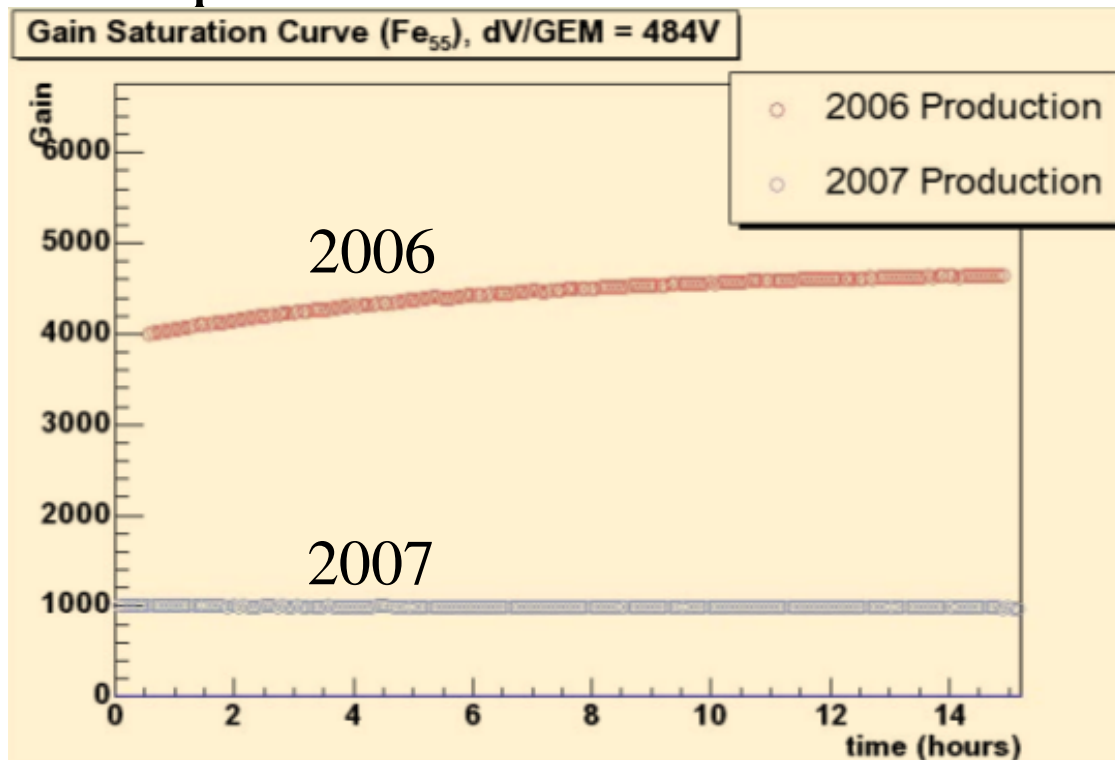
Gain in a pristine GEM

- ▶ Calculations predict that G_{tot} and G_{eff} rise with increasing inner hole diameter.
- ▶ G_{eff} rises mainly because the losses of incoming electrons diminish;
- ▶ G_{tot} rises because the exit electrode becomes more accessible.



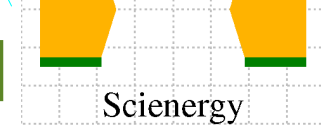
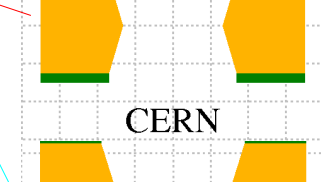
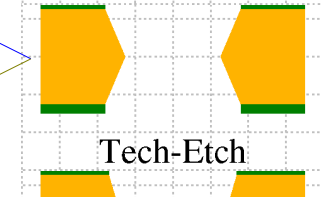
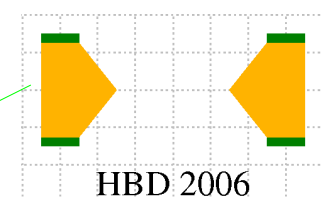
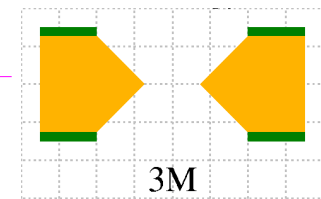
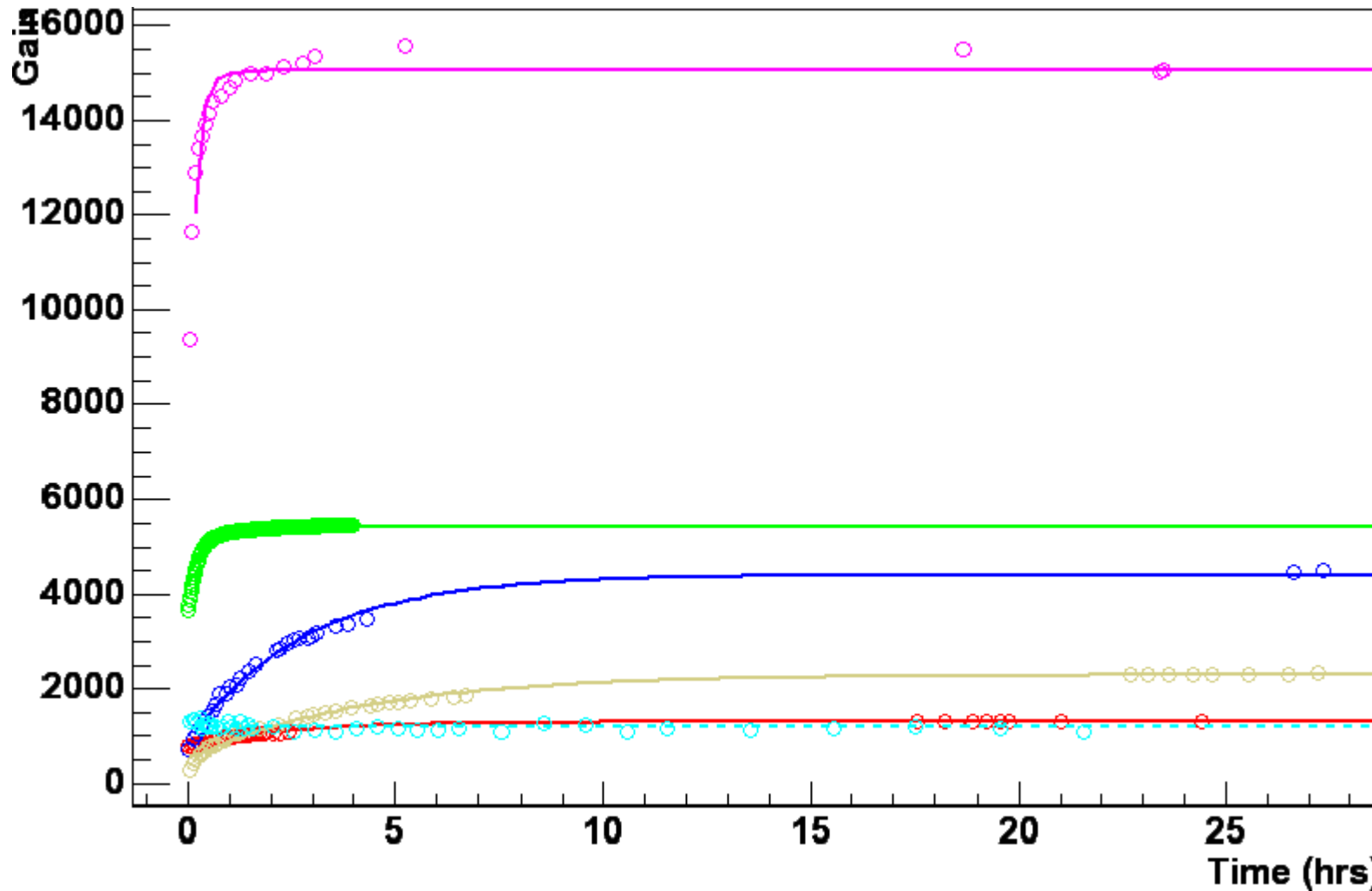
HBD data

- ▶ Measurements for 2 triple GEMs with different hole shape shows that smaller holes lead to *larger* gain !



- ▶ [W. Anderson *et al.* 10.1109/NSSMIC.2007.4437147]

GEMs of various manufacturers



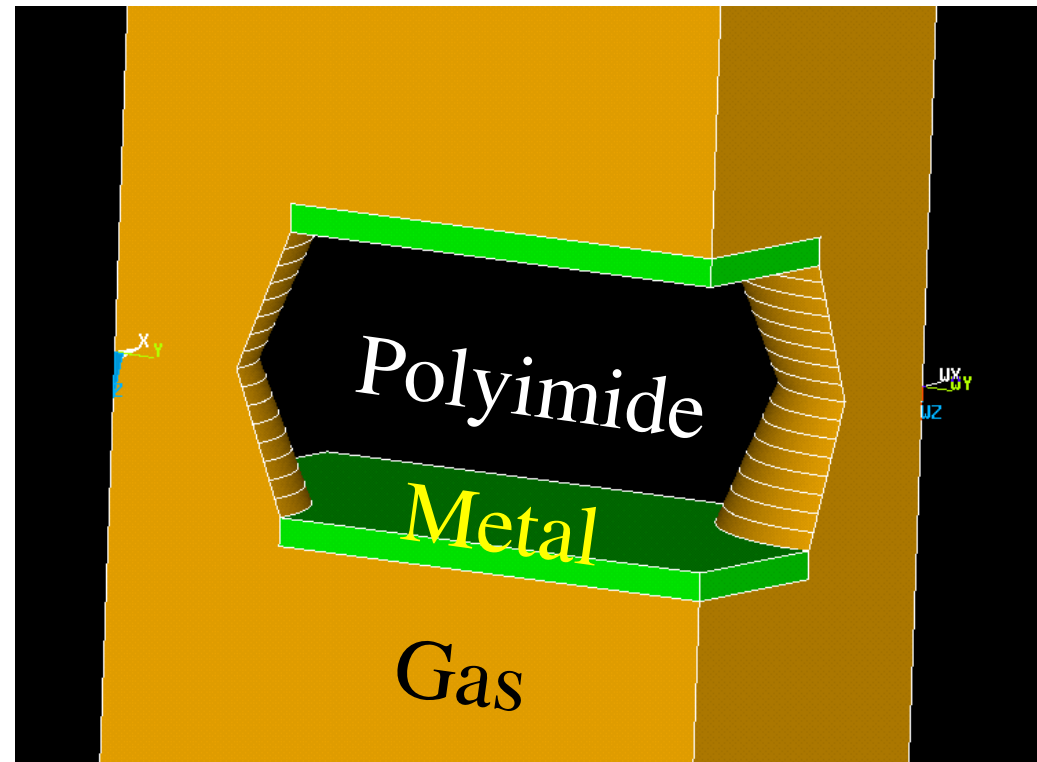
► [B. Azmoun *et al.* 10.1109/NSSMIC.2006.353830]

Surface charge

- ▶ GEMs violate the 1st law of gas-based detectors: active gas is in contact with an insulator.
- ▶ Electrons and ions will therefore land on the insulating material.
- ▶ Polyimide as used in GEMs is an extraordinarily good insulator: once on the surface, charge stays there.

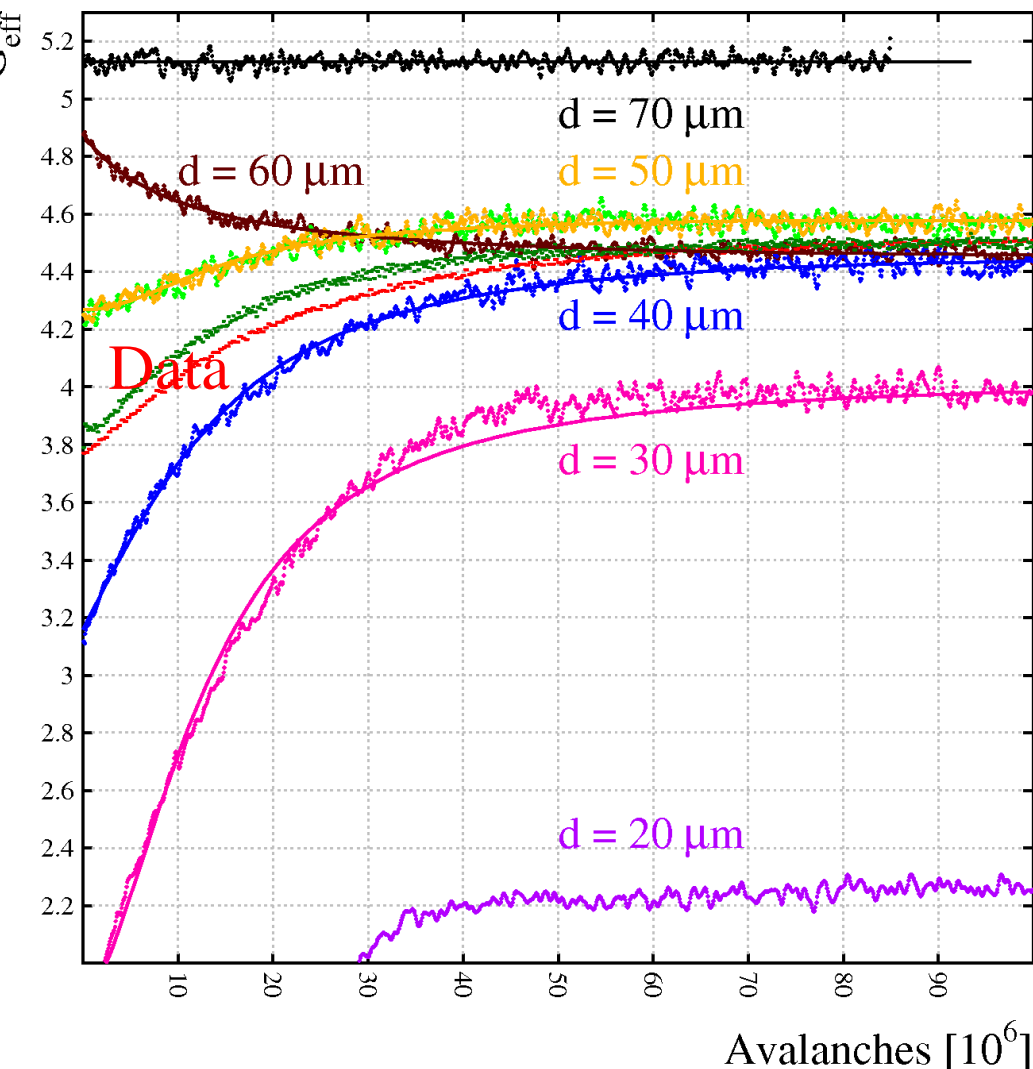
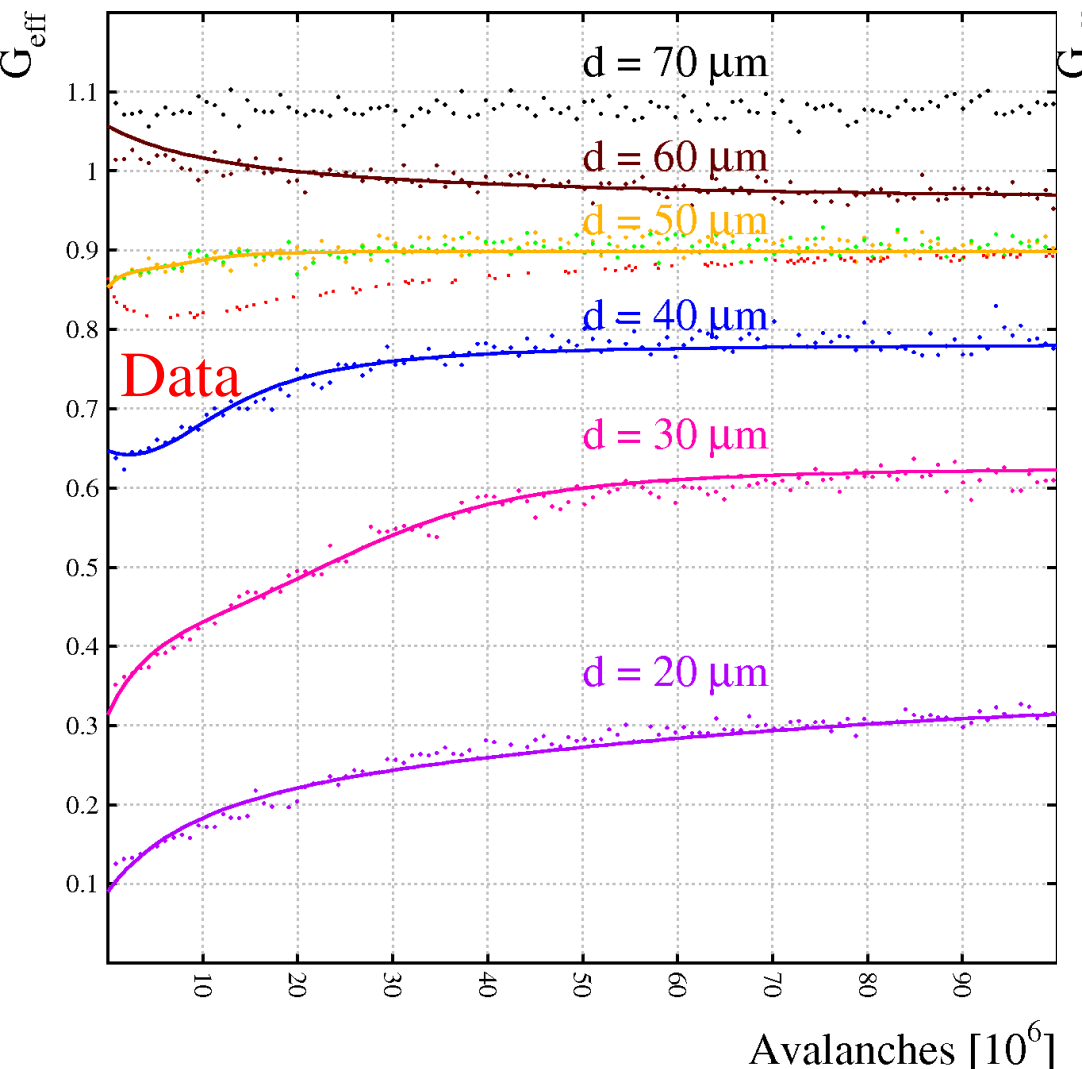
GEMs with surface charge

- ▶ The polyimide surface area inside the holes is sliced.
- ▶ Start: uncharged GEM;
- ▶ Iterate: run avalanches; histogram electron and ion deposition patterns; add surface charges and recalculate the field;
- ▶ Convergence: electron and ion deposits balance.

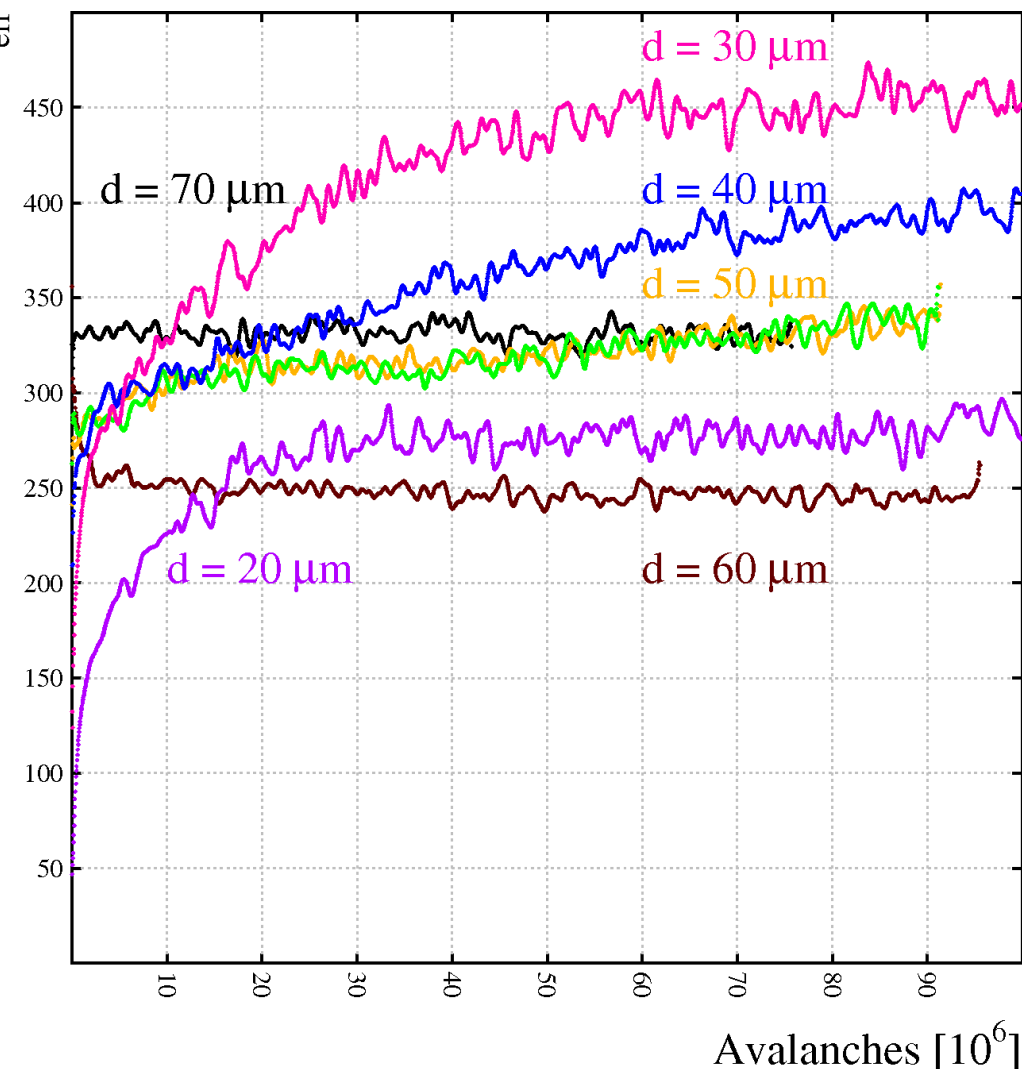
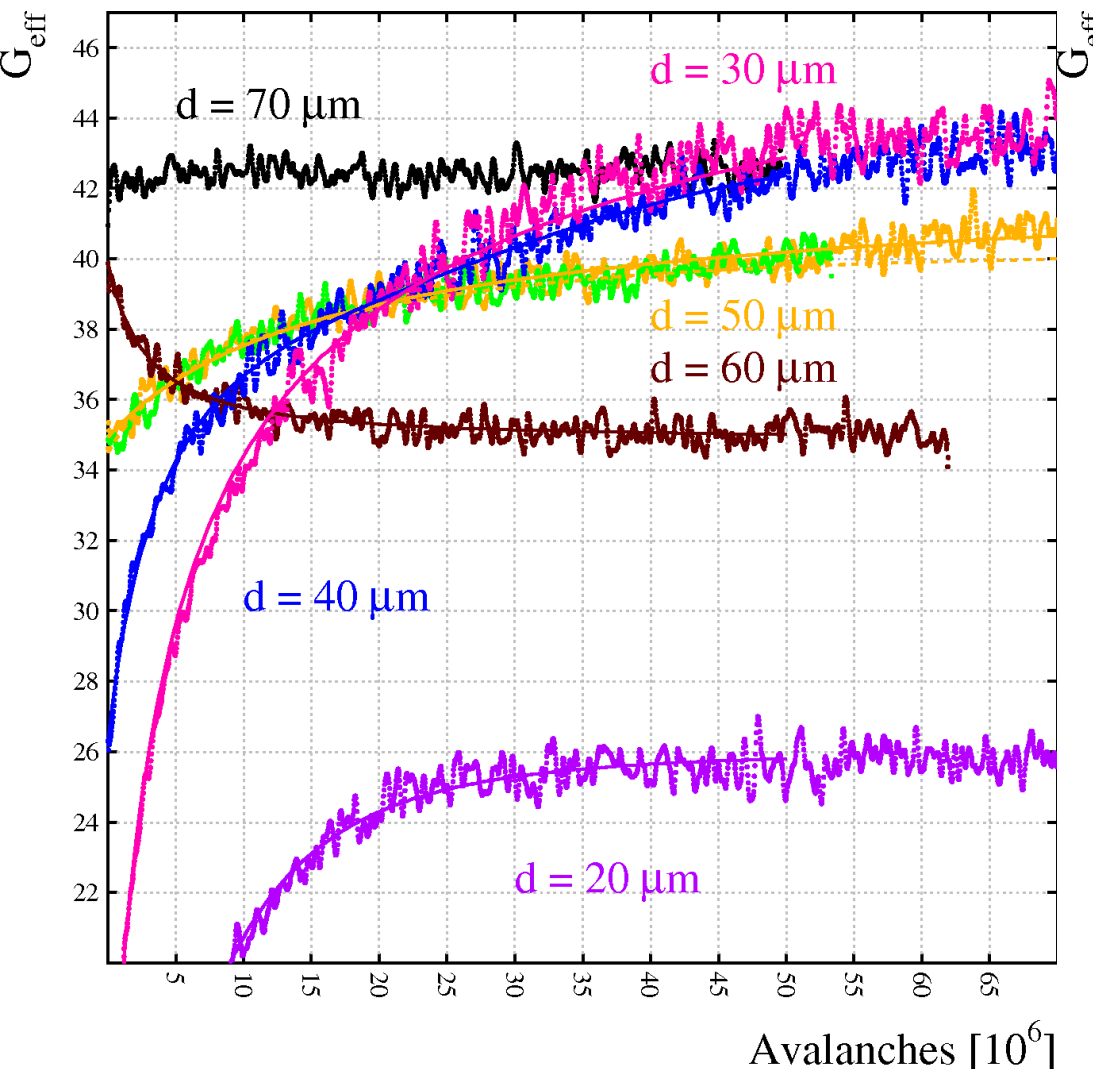


See the poster of Pedro Correia

$V_{\text{GEM}} = 220 \text{ V}$ and $V_{\text{GEM}} = 300 \text{ V}$

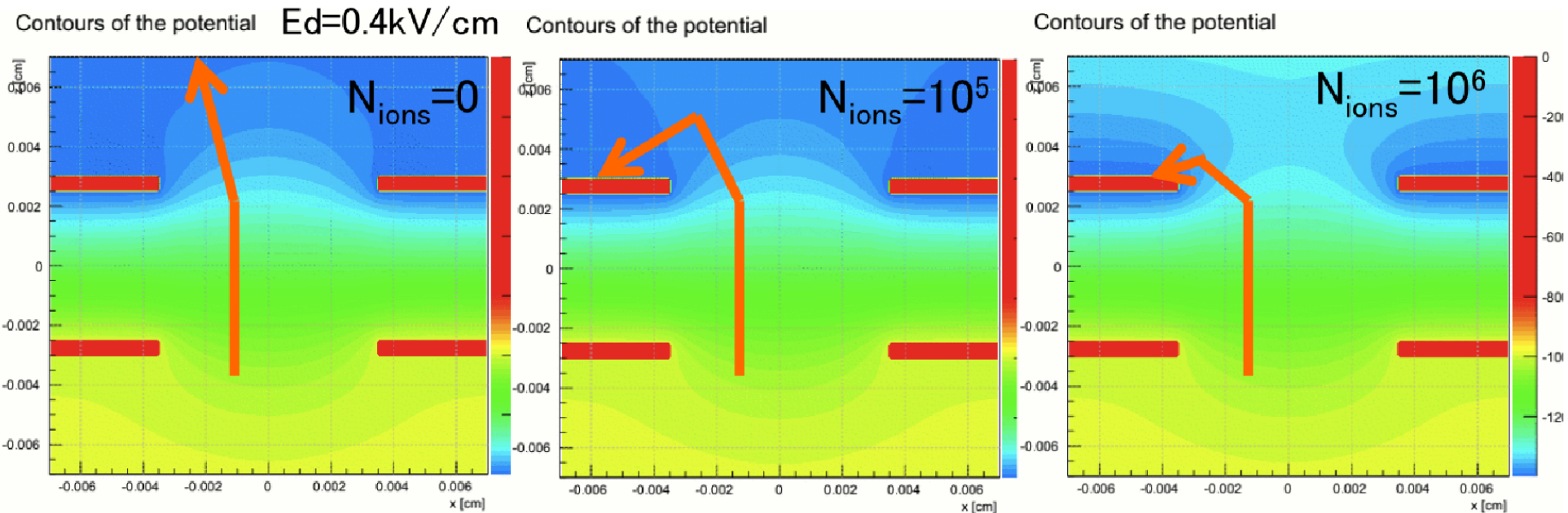


$V_{\text{GEM}} = 400 \text{ V}$ and $V_{\text{GEM}} = 500 \text{ V}$



Space-charge simulations: Method

- ▶ Slice the space in drift direction by $100 \mu\text{m}$
- ▶ Uniformly distribute ions in space $z \in [Z, Z + 100\mu\text{m}]$
- ▶ Calculate the field by ANSYS and evaluate gain/IBF by Garfield++
- ▶ Example of the field around GEM1 with $N_{ions}=0, 10^5, 10^6$ with $E_{drift}=0.4\text{kV/cm}$. less IBF with huge N_{ions} ?



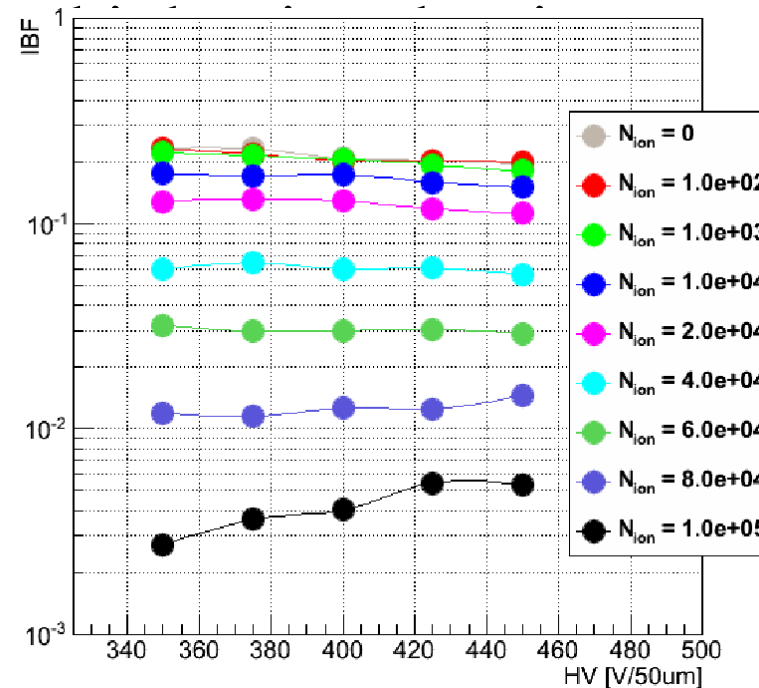
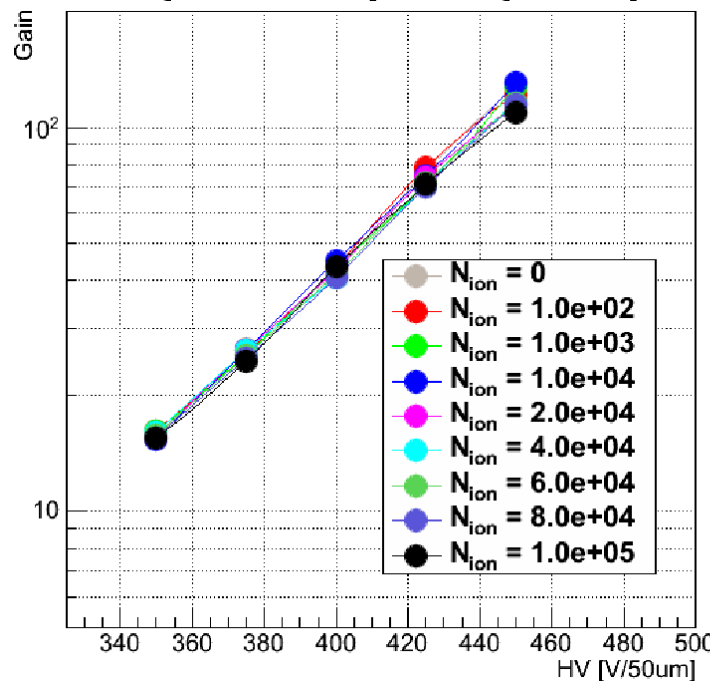
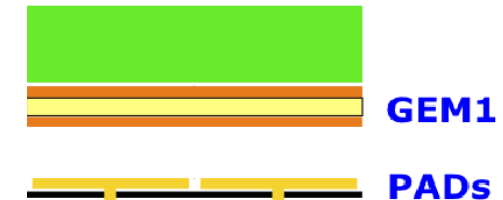
Space-charge above a single GEM

• • • • • • • • • • • Drift plane

- Ions at $z \in [0, 100 \mu\text{m}]$ above the GEM;

$$E_{\text{dr}} = 400 \text{ V/cm}; \text{Ar}/\text{CO}_2 \text{ 70/30};$$

- Gain: Does not depend on the ion density;
- IBF: Onset of decrease at $\sim 10^4$ ions/hole,



Note: N_{ions} is expressed in ions / $\frac{1}{2}$ hole

Now and next

- ▶ Present situation:
 - ▶ “drift line integration” is not appropriate in MPGDs;
 - ▶ microscopic electron transport works, albeit slowly;
 - ▶ a multitude of molecular processes play a role;
 - ▶ simulation moves from mathematics to physics;
 - ▶ progress relies on dedicated precision measurements.
- ▶ The next challenges
 - ▶ ion transport;
 - ▶ signals with resistive layers;
 - ▶ photon processes.